ELSEVIER

Coordination Chemistry Reviews
176 (1998) 373–406

COORDINATION CHEMISTRY REVIEWS

Synthetic applications of p block metal dimethylamido reagents

Michael A. Beswick, Dominic S. Wright*

Chemistry Department, Cambridge University, Lensfield Road, Cambridge CB2 1EW, UK

Received 4 December 1997; accepted 24 December 1997

Contents

Abstract

The reactions of dimethylamido p block metal reagents with primary amines (RNH_2) and primary amido and phosphido alkali metal complexes ([REHM]; E = N, P; M = alkali metal) furnish direct routes to a range of imido and phosphinidene compounds. In particular, novel p block metal polyimido and phosphinidene anions are readily accessible from

* Corresponding author. Tel.: +44 1223 336333; fax: +44 1223 336362; e-mail: dsw1000@phx.cam.ac.uk

PII S0010-8545(98)00126-X

these reactions. These function as versatile ligands to a variety of main group and transition metals, giving a structured approach to the assembly of heterometallic complexes containing a broad spectrum of mixed-metal stoichiometries. This review describes the synthetic applications of p block metal dimethylamido reagents to a range of p block metal compounds and the structures and reactivities of the imido and phosphinidene complexes produced.

Keywords: Dimethylamido; p block; Cages; Imido; Phosphinidene

1. Introduction

Metallo–organic complexes of p block elements (alkloxides, amides, phosphides, etc., of Groups 13–15) have attracted considerable attention in the past two decades owing to their potential applications as molecular, single-source precursors to a variety of technologically important materials (for examples of Group 13 precursors, see Cowley and Jones [1] and Wells [2]). However, in general there are a limited number of synthetic approaches to these species (for examples involving Ga and Al, see Paver et al. [3]). Most common strategies are: (i) the transmetallation of p block metal halides with alkali metal alkoxides, amides and phosphides; (ii) metallation of organic acids with p block organometallics; and (iii) reaction of silyl amides and phosphides (etc.) with p block halides (leading to the elimination of thermodynamically stable silyl halides). There are several obvious problems with these existing routes. In particular, the lower polarity of p block metal–carbon bonds makes the organometallics considerably less reactive than those of the alkali metals [4,5] and frequently transmetallation of metal halides can give rise to mixtures of products or poor selectivity. In addition, although imido and phosphinidene compounds of Group 13 metals (containing RN^{2-} and RP^{2-} functionality) are known [3], such compounds are rare for other metals in the p block. This situation largely stems from the very low basicity of Group 14 and 15 organometallics, which will not readily doubly-deprotonate primary amines or phosphines, and from the lack of stable alkali metal imido and phosphinidene precursors for transmetallation (for a rare example, see Armstrong et al. [6]).

With this background in mind, a principal aim in our initial studies was to develop a general approach to imido and phoshinidene complexes of p block elements [7]. Earlier literature showed that the dimethylamido metal complexes of Groups 14 and 15 are readily accessible by transmetallation of the appropriate metal halides with $[LiNMe_2]$ and the limited studies of the reactions of $[Sb(NMe_2)_3]$ with simple organic acids (amides and secondary amines) illustrated that this species is a potent base [8–12]. This reactivity is markedly different from commercially available organo–Group 15 complexes (such as $[Ph_3Sb]$) which are relatively unreactive towards organic acids. It transpires that such dimethylamido reagents are highly effective in the low-temperature synthesis of imido and phosphinidene complexes of the p block metals, a strategy which lead to the preparation of a new

class of imido and phosphinidene metal ligand systems and to the logical assembly of a variety of heterometallic cage compounds. This review concerns the development of this area and describes the tremendous synthetic potential of these reagents in the preparation of a diverse range of molecular arrangements.

2. Group 15 systems

2.1. Reactions of $[SbCl_x(NMe_2)_{3-x}]$ with primary amines

As noted in the introduction, previous synthetic studies with $[Sb(NMe_2)_3]$ had involved simple organic substrates containing one reactive proton. The focus for our preliminary work was the exploration of reactions with primary amines, in an attempt to provide a simple route to imido Sb(III) complexes. The low-temperature reactions of $[E(NMe_2)_3]$ (E = Sb, Bi) with a variety of primary amines (RNH_2; R = 4-methylpyridin-2-yl, $C_6H_2(OMe)_3$-3,4,5 [13], C_6H_4(1-OMe), Bu^t [14]) give similar centrosymmetric imido dimers $[Me_2NSn(\mu\text{-}NR)]_2$, containing central E_2N_2 cores and with terminal NMe_2 groups on each metal centre [Eq. (1)]. The key point illustrated by these initial reactions is that double-deprotonation of primary amines occurs irrespective of the organic group (R) and that conjugative stabilisation within the imido anion formed is not required to enhance the reactivity of the amine. This reactivity pattern can be compared to that of organoalkali metal reagents (such as Bu^nLi) which will normally only singly-deprotonate primary amines except where a stabilised imido system is generated [6]). The structures of $\{Me_2NSb[\mu\text{-}N(4\text{-methylpyridin-2-yl})]\}_2$ (**1**) and $\{Me_2NSb[\mu\text{-}NC_6H_2(OMe)_3\text{-}3,4,5]\}_2$ (**2**) (Fig. 1) [13] illustrate a further common feature of these compounds found where organic groups containing additional functionality are present. In **1** the pyridyl rings are in the same plane as the Sb_2N_2 core and the presence of intramolecular pyridyl-N$\cdots$Sb interactions results in the pivoting of the pyridyl substituents towards their respective metal centres. However, the remote functionality present in the $NC_6H_2(OMe)_3$-3,4,5 groups of **2** means that such intramolecular bonding cannot occur. Instead, the aromatic rings tilt out of the plane of the Sb_2N_2 core and intermolecular Sb$\cdots$O interactions link the dimeric units into a loosely-associated sheet structure.

Previous studies of $[Bu^tSb(\mu\text{-}NBu^t)]_2$ illustrated that an intramolecular equilibrium involving the *cis* and *trans* dimers occurs in solution [15]. Similar *cis–trans* equilibria are found for the majority of $[Me_2NSb(\mu\text{-}NR)]_2$ dimers. However, the presence of intramolecular interactions in **1** has a profound effect on the interconversion of the *cis* and *trans* isomers and favours the retention of a *trans* arrangement [13]. In this respect, the structure of $\{(Me_2N)Sb[\mu\text{-}N(Dipp)]\}_2$ (**3**) (Dipp =

$$2[Sb(NMe_2)_3] + 2RNH_2 \longrightarrow [Me_2NSn(\mu\text{-}NR)]_2 + 4Me_2NH \quad \ldots(1)$$

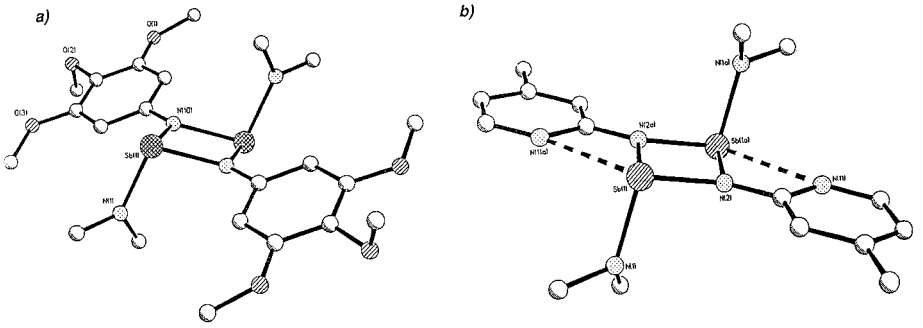

Fig. 1. The crystal structures of (a) $\{Me_2NSb[\mu\text{-}N(4\text{-methylpyridin-2-yl})]\}_2$ (**1**) and (b) $\{Me_2NSb[\mu\text{-}NC_6H_2(OMe)_3\text{-}3,4,5]\}_2$ (**2**).

2,6-$Pr^i_2C_6H_3$-) [16] is particularly worthy of note (Fig. 2). The presence of extremely sterically demanding bridging groups and the steric confrontation between the Pr^i substituents and the terminal NMe_2 groups favours a unique *cis* dimer conformation in the solid state, containing a puckered Sb_2N_2 core. Variable-temperature ^1H NMR studies illustrate that the *cis* conformation is retained in solution at and below room temperature.

The reactivities of $[SbCl_x(NMe)_{3-x}]$ ($x = 1$ or 2), formed by equilibration of $[Sb(NMe_2)_3]$ and the appropriate stoichiometric quantity of $SbCl_3$, are similar to that of $[Sb(NMe_2)_3]$. The reactions of EtOH with $[SbCl_2(NMe_2)]$ [Eq. (2)] and Bu^tNH_2 [Eq. (3)] with $[SbCl(NMe_2)_2]$ give the dimers $[SbCl_2(Me_2NH)(\mu\text{-}OEt)]_2$

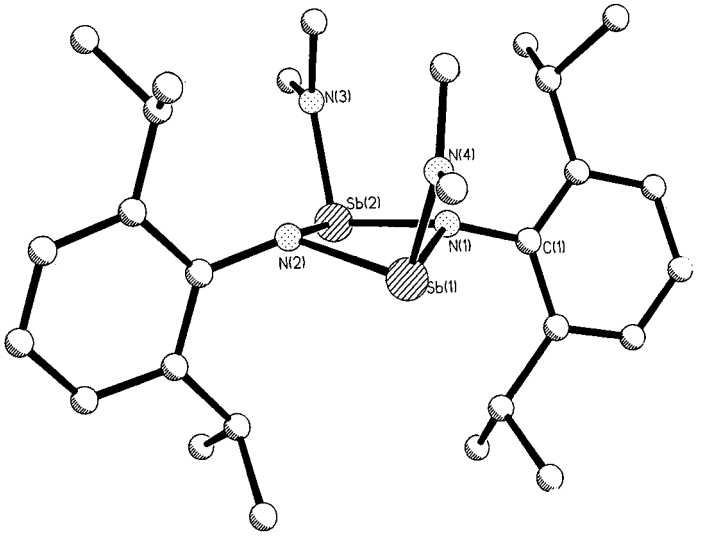

Fig. 2. The crystal structure of the puckered *cis* dimer $\{(Me_2N)Sb[\mu\text{-}N(Dipp)]\}_2$ (**3**).

$$2[Sb(NMe_2)Cl_2] + 2EtOH \longrightarrow [SbCl_2(Me_2NH)(\mu\text{-}OEt)]_2 \quad \textbf{3} \quad \ldots(2)$$

$$2[Sb(NMe_2)_2Cl] + 2^tBuNH_2 \longrightarrow [SbCl(Me_2NH)(\mu\text{-}N^tBu)]_2 + 2Me_2NH \quad \textbf{4} \quad \ldots(3)$$

(**4**) and $[SbCl(Me_2NH)(\mu\text{-}NBu^t)]_2$ (**5**) (Fig. 3), respectively [17]. However, the presence of chlorine substituents increases the Lewis acidity of the Sb(III) centres and gives rise to far more extensive intermolecular association in these systems than occurs in $[Me_2NSb(\mu\text{-}NR)]_2$ dimers. This greater Lewis acidity also has the important result that the Me_2NH produced as a byproduct in these reactions functions as a ligand to the Sb(III) centres in **4** and **5**.

2.2. Heterometallic cage complexes of Group 15

The high reactivity of Bi and Sb dimethylamido reagents illustrated in initial studies can be used to particular advantage when one considers the far lower reactivity of organolithium compounds (RLi) with primary amines and phosphines (REH_2; E = N, P). The reactions of these organic acids with RLi followed by condensation with dimethylamido reagents in principle provides a way of building heterometallic compounds. This scenario is shown schematically in Fig. 4.

This step-wise metallation process in fact proves highly versatile in the preparation of a range of novel heterobimetallic Sb and Bi/Li cage complexes. By using various dimethylamido Sb(III) reagents different anion arrangements can be as-

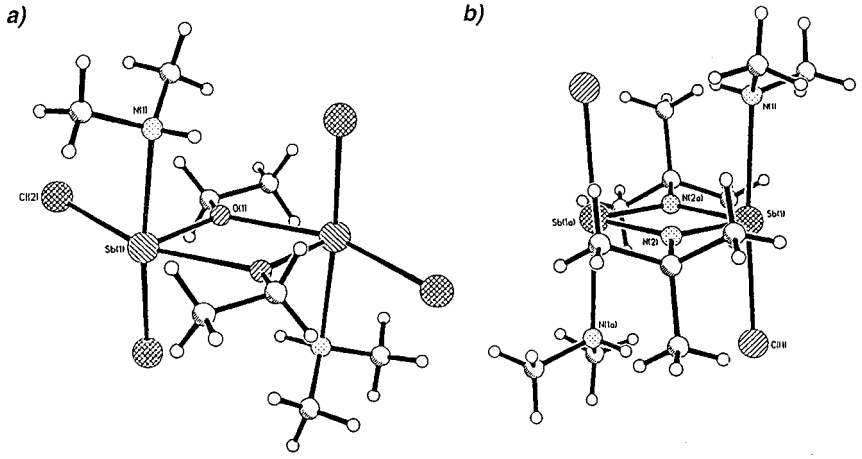

Fig. 3. The crystal structures of (a) $[SbCl_2(Me_2NH)(\mu\text{-}OEt)]_2$ (**4**) and (b) $[SbCl(Me_2NH)(\mu\text{-}NBu^t)]_2$ (**2**).

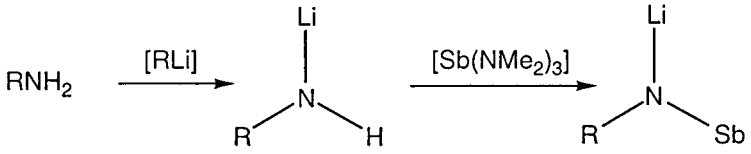

Fig. 4. Sequential double deprotonation of a primary amine.

sembled in a predictable way. Heterobimetallic alkali metal cage complexes containing $\{[(R^1R^2N)Sb(NR)]_2Sb\}^-$ monoanions, $[Sb_2(NR)_4]^{2-}$ dianions and $[Sb(NR)_3]^{3-}$ trianions are the major classes of these 'polyimido' ligands which have been prepared (Fig. 5). These species have proven to be robust multidentate ligand systems. Their transmetallation and co-complexation reactions with transition metal and main group metal salts provides a strategy for the assembly of heterometallic and complexes containing a variety of mixed-metal stoichiometries. The syntheses of these anionic ligands and their coordination chemistry is discussed in the following sections.

2.2.1. Polyimido-antimonates containing $[Sb(ER)_3]^{3-}$ trianions (E = N, P)

The simplest step-wise metallation reaction is that of the reaction of a primary amido or phosphido lithium complex, $[REHLi]_n$ (E = N, P), with $[Sb(NMe_2)_3]$ (1:3 monomer equivalents) [Eq. (4)]. These reactions lead to heterobimetallic $[Sb_2E_6Li_6]$ cages containing $[Sb(ER)_3]^{3-}$ trianions (type *III*, Fig. 5). The first example of this type to be prepared was that of $\{[Sb(NCH_2CH_2Ph)_3]Li_3 \cdot THF\}_2$ (**6**) [18]. The low-temperature X-ray crystal structure of **6** (Fig. 6) shows it to be a 14-membered

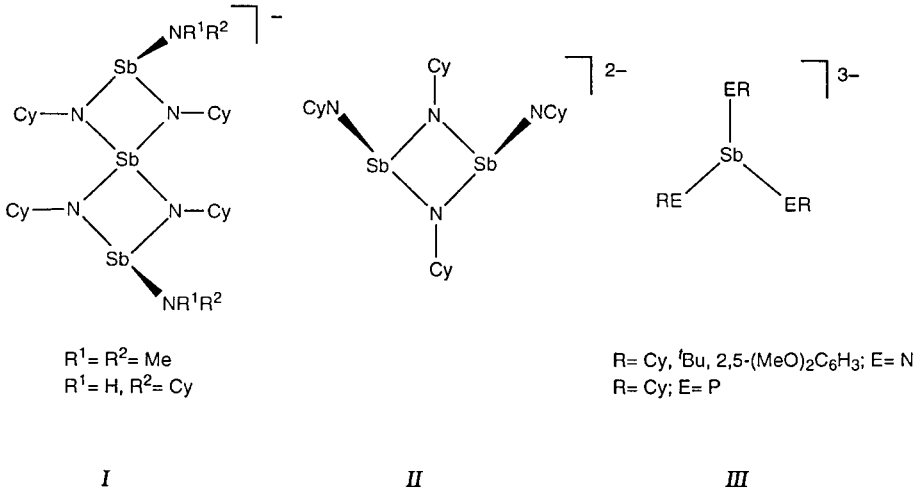

Fig. 5. Schematic representation of the imido Sb(III) anions generated by stepwise metallation.

$$[Sb(NMe_2)_3] + 3[RNHLi] \longrightarrow {}^1/_2[\{Sb(NR)_3\}_2Li_6] + 3Me_2NH \quad ...(4)$$

cage constructed from the association of two $[Sb(NCH_2CH_2Ph)_3]^{3-}$ trianions by six Li^+ cations. Alternatively the complex can be regarded (conceptually) as an N_6Li_6 'stack' structure [4,5] capped at the open N_3Li_3 faces by two Sb(III) centres. In the core of **6**, four of the lithium centres are involved in agostic *ortho* $(C-H)\cdots Li$ interactions with the phenyl rings of adjacent $PhCH_2CH_2-$ groups, with the other two lithium atoms being complexed by THF. The agostic interactions in **6** are typical of those found in amido–lithium compounds, such as in $\{[PhCH_2]_2NLi\}_3$ [19,20]. Similar core geometries have been observed previously in the structures of $\{[(Pr^i_3Si)AsLi]_3GeBu^t\}_2$ [21–22] and $[(RNLi)_3SiR']_2$ (R = Me_3Si, R′ = Me, Bu^t, Ph [23]; R = Bu^t, R′ = Ph [24]; R = Me, R′ = Bu^t [25]).

On the basis of the apparent similarity between the cyclic octameric ladder structure of $[Bu^tN(H)Li]_8$ [26] and the hexameric 'ladder' core of **6**, it was recently proposed that the structure of **6** is templated by the rigid cyclic ladder structure of $[PhCH_2CH_2N(H)Li]_n$ (which was postulated to have a cyclic hexameric structure, $n = 6$). According to this theory these species are composed of rigid N_6Li_6 'ladders' in which Sb^{3+} ions are bound 'to the bed of N atoms on each side of the core,...akin to the way in which metal cations fit macrocyclic crown–ether holes'. However, in the reaction of $[Sb(NMe_2)_3]$ with $[Bu^tN(H)Li]_8$ the octameric core of the primary amido lithium precursor is not retained (Fig. 7). The product of this reaction is the cage $\{[Sb(NBu^t)_3]_2Li_6\}$ (**7**), having a similar structural arrangement

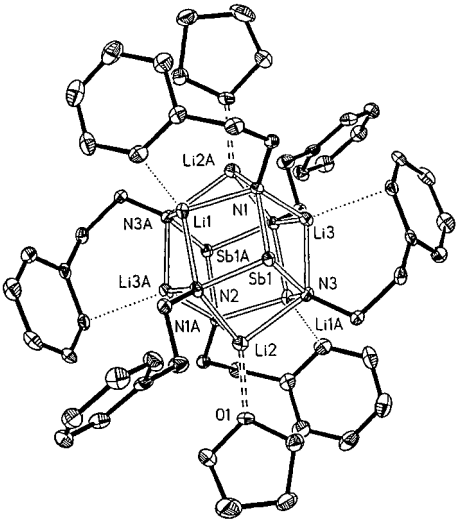

Fig. 6. The crystal structure of $\{[Sb(NCH_2CH_2Ph)_3]Li_6 \cdot THF\}_2$ (**6**).

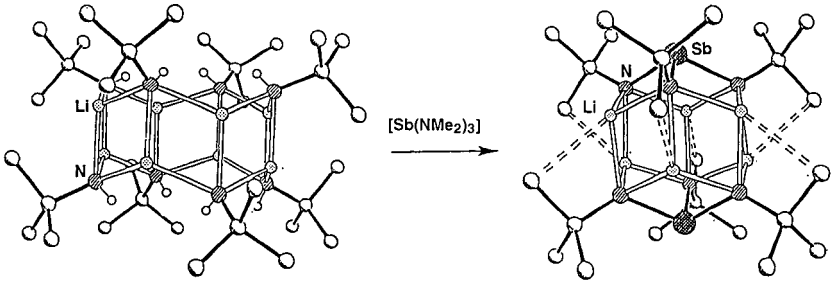

Fig. 7. Reaction of $[Bu^tN(H)Li]_8$ with $[Sb(NMe_2)_3]$, giving **7**.

to **6** [27]. This finding illustrates the key point that the formation and structures of all of these $[Sb_2N_6Li_6]$ cages is dominated by the bonding requirements and valence of the Sb(III) centres and that the $[N_6Li_6]$ subunits merely perform an associative role.

Stressing the dominance of the $[Sb(NR)_3]^{3-}$ anion units in these systems, in $\{Sb[N(2,4\text{-dmp})]_3\}_2Li_6 \cdot 2THF$ (**8**) [27] [2,4-dmp = 2,4-$(MeO)_2C_6H_3$] (Fig. 8) the extensive intramolecular solvation of all of the Li^+ cations of the core by the *ortho*-MeO substituents of the organic ligand results in major distortion of the N_6Li_6 substructure. The two-MeO groups of each of the $\{Sb[N(2,4\text{-dmp})]_3\}^{3-}$ trianions straddle the N_6Li_6 belt of the core, engaging the lithium cations associated with the other trianion unit (cf. **6** in which the agostic contacts occur within each half of the core). Each of the Li^+ cations of the $\{Sb[N(2,4\text{-dmp})]_3\}^{3-}$ halves have different coordination environments. Two of the 2,4-dmp ligands of each of the trianions adopt similar monodentate bridging modes and the other a μ–O mode. For Li(1), the coordination of the O atom of a monodentate ligand and the weak attachment of a μ–O bridging ligand gives this centre a pseudo five coordinate geometry. A similar five coordinate arrangement is also attained for Li(3), being coordinated to a μ–O ligand and a THF molecule. Li(2) is coordinated solely by a monodentate ligand resulting in a pseudo tetrahedral environment. Despite the large distortions in the N_6Li_6 framework [particularly at Li(3)] resulting from this intricate pattern of solvation, there is little change in the geometry of the $[Sb(NR)_3]^{3-}$ trianion units of **8** compared to the trianions of **6** and **7**.

A surprising structural feature recently observed in these trianion systems is the solvation of the N_6Li_6 cores by Me_2NH, produced as a byproduct in the reactions of $[Sb(NMe_2)_3]$ with certain primary amido and phosphido lithium complexes. In $\{[Sb(NCy)_3]_2Li_6 \cdot 2HNMe_2\}$ (**9**) [27] (Fig. 9) two Me_2NH ligands occupy equivalent positions to the THF ligands which solvate the core in **6**. In the phosphinidene cage $[Sb(PCy)_3]_2Li_6 \cdot 6HNMe_2$ (**10**) [28] all of the Me_2NH produced from the 1:3 reaction of $[Sb(NMe_2)_3]$ with [CyPHLi] solvates the Li^+ cations (Fig. 10a). The difference in the extents of solvation of the cores of **9** and **10** presumably stems from the presence of shorter N–Li bonds in **9**, resulting in greater steric shielding of the Li^+ cations. Solvation of Li^+ by labile protic ligands like Me_2NH (a gas

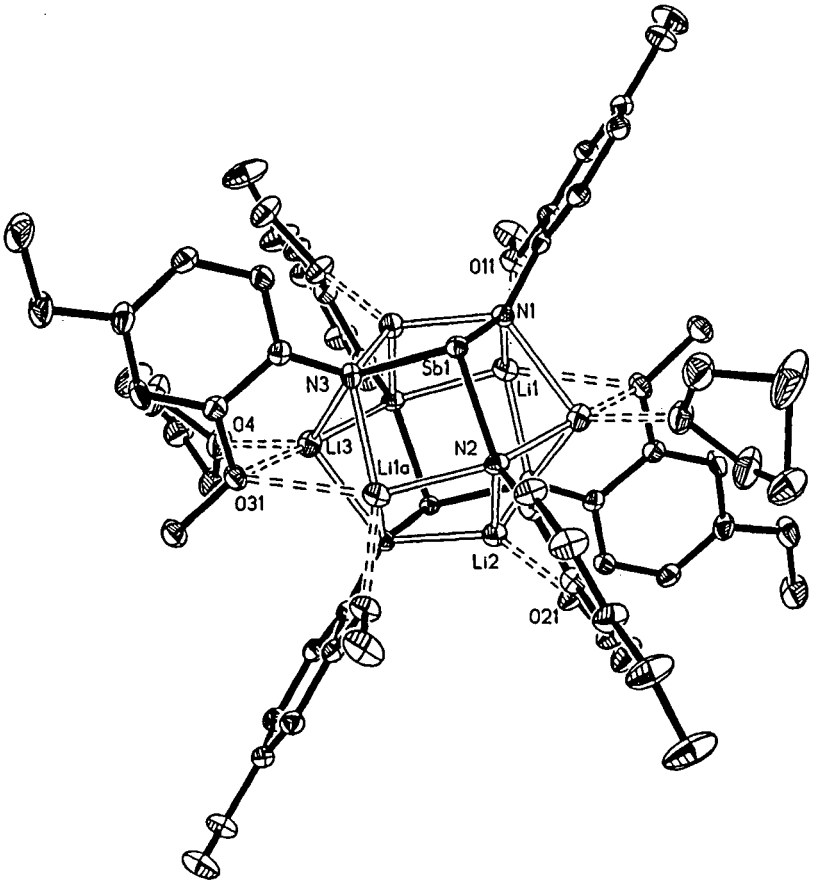

Fig. 8. The crystal structure of $\{Sb[N(2,4\text{-dmp})]_3\}_2Li_6 \cdot 2THF$ (**8**).

above 7°C) is extremely rare. Although this solvation is removed by placing both complexes under reduced pressure, it is comparatively robust in the solid complexes at room temperature (particularly in **9**). The presence of NMR-active ^{31}P in the core of **10** allows potential dynamic processes occurring in the $[Sb_2P_6Li_6]$ core to be investigated. In the ^{7}Li NMR spectrum a binomial septet ($^{1}J_{31_{P-7Li}} = 14$ Hz) occurs as a result of the coupling of all of the Li^+ cations to the P atoms of two *intact* trianions (203–298 K) (Fig. 10b). Semi-empirical PM3 calculations indicate that interchange of the six Li^+ cations occurs by a dynamic ('carousel') process, analogous to that observed for $[Me_2Si(NSiMe_3)_2]_2InLi$ in solution [29], in which the Sb(III) centres are not involved. The ^{31}P NMR chemical shift (−263.5 ppm) is vastly different to that observed for $\{(2,4,6\text{-}Bu^t_3C_6H_2)P = Sb[CH(SiMe_3)_2]\}$ (600 ppm) [30], reflecting the development of the negative charge on the P centres of **10**. The fluxionality of the Li^+ cations in **10** indicates that, like the $[Sb(NR)_3]^{3-}$

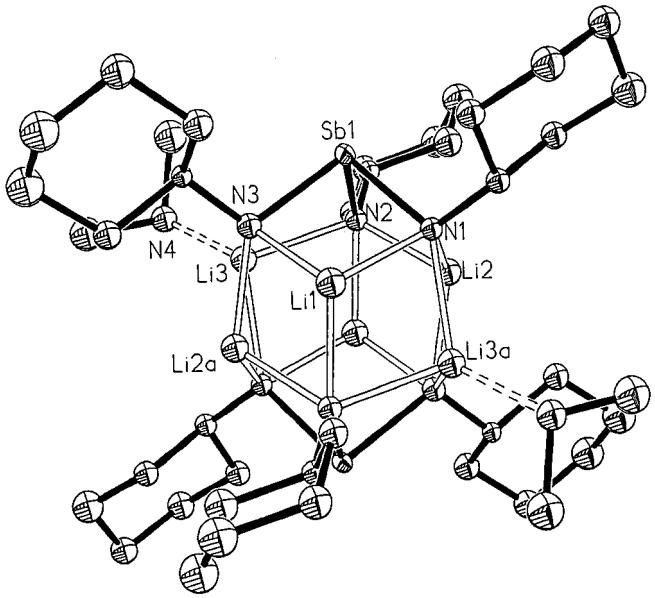

Fig. 9. The crystal structure of $\{[Sb(NCy)_3]_2Li_6 \cdot 2HNMe_2\}$ (**9**).

trianions of **6**–**8**, the $[Sb(PR)_3]^{3-}$ trianion is the robust chemical constituent of this complex. The fact that the structure of the phosphido lithium precursor has no bearing on the structure of **10** is further stressed by a comparison between its cyclic ladder core and the polymeric ladder structure found for the precursor $[CyPHLi \cdot THF]_\infty$ [31]. Complex **10** is only the second example of a phosphinidene complex of Sb or Bi to be structurally characterised, the first being $[SbP(2,4,6\text{-}Bu^t_3C_6H_2)]_2$ [32].

As is evident from the structural and spectroscopic properties of lithium complexes containing $[Sb(ER)_3]^{3-}$ trianions (E = N, P), these units (not the E_6Li_6 substructures) are the robust chemical entities in these systems. This is also evident from their ligand behaviour. The addition of the main group or transition metal sources gives products which retain the trianion framework. Two possible reaction types have been identified, (i) transmetallation, involving exchange of the Li^+ cations for another metal; and (ii) co-complexation, in which the species added incorporates itself into the original complex.

The reaction of $\{[Sb(NCy)_3]_2Li_6 \cdot 2HNMe_2\}$ (**9**) with $[Cp_2Pb \cdot TMEDA]$ [33] eliminates $[CpLi \cdot TMEDA]$ and gives the Pb(II)/Sb(III) cage $\{[Sb(NCy)_3]_2Pb_3\}$ (**11**) [Eq. (5)], Fig. 11) [34]. The crystal structure determination shows that **11** exist as an 11-membered cage containing an $[Sb_2Pb_3]$ metal core held together by six imido groups. Clearly the $[Sb_2N_6Pb_3]$ core is held together by N–Sb and N–Pb bonding, rather than there being any significant metal ⋯ metal interactions. However, it is interesting to note that the trigonal bipyramidal $[Sb_2Pb_3]$ metal fragment can be viewed conceptually as a $n + 1$ (Wade's rule) polyhedron.

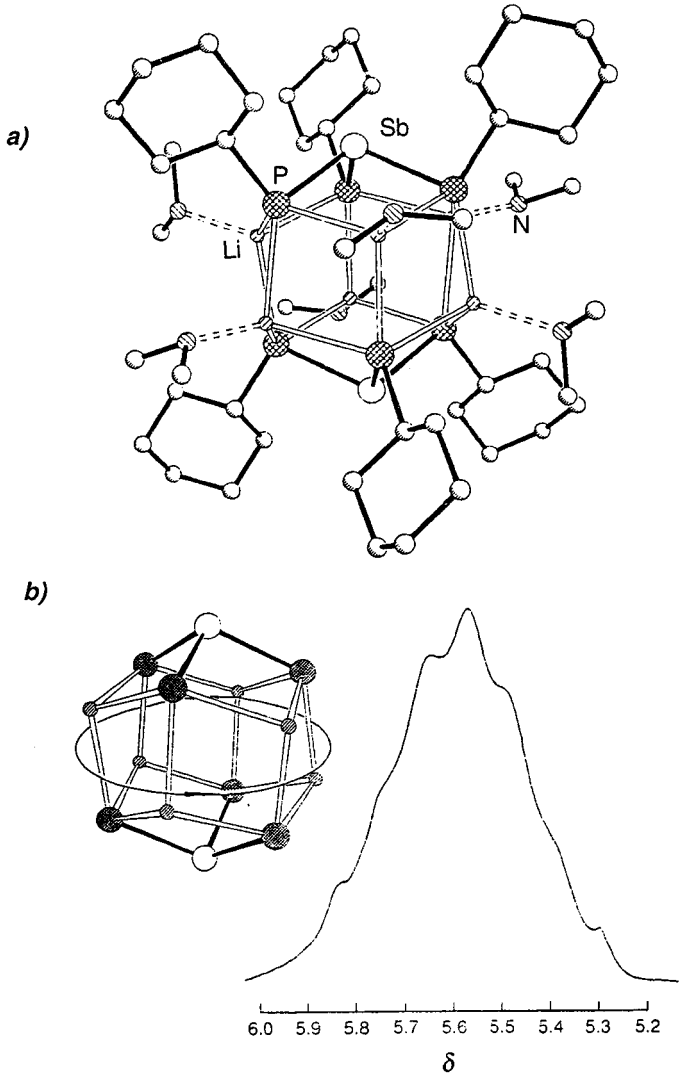

Fig. 10. (a) The crystal structure of $[Sb(PCy)_3]_2Li_6 \cdot 6HNMe_2$ (**10**) and (b) the 'dynamic carousel' process.

Co-complexation rather than transmetallation occurs when **9** is mixed with $KOBu^t$. The crystallographic study shows that the product is the remarkable trimetallic cage complex $\{[Sb(NCy)_3]_2(KOBu^t)_3\}$ (**12**) [35], in which the cage expansion of the bimetallic precursor from a 14- to a 20-membered polyhedron has occurred (Fig. 12). The cage structure consists of a central planar $[K(\mu_2\text{-}OBu^t)]_3$ ring which is sandwiched between the *intact* halves of the parent compound **9**. This unusual co-complexation reaction is thought to be driven by the formation of

$$[\{Sb(NCy)_3\}_2Li_6].2Me_2NH + 3[Cp_2Pb] \xrightarrow{-2Me_2NH} [\{Sb(NCy)_3\}_2Pb_3] + 6[CpLi] \quad \ldots(5)$$

11

strong Li–O bonds in the product and by the relief in the strain brought about by expanding the 14-membered cage to a 20-membered cage.

2.2.2. Polyimido-antimonates and bismuthates containing $[E_2(NR)_4]^{2-}$ dianions (E = Sb, Bi)

The dimeric complexes $[(Me_2N)Sb(\mu\text{-}NR)]_2$, discussed in Section 2.1, contain terminal NMe_2 groups which are potentially reactive towards primary amido lithium complexes. The condensation reaction between $[Me_2NSb(\mu\text{-}NCy)]_2$ and $[CyNHLi]_n$ (1:1 monomer equivalents) in non-donating solvents yields $[Sb_2(NCy)_4]_2Li_4$ (**13**) in which the rational assembly of an $[Sb_4N_8Li_4]$ cage is achieved (Fig. 13) [36]. This structural arrangement is similar to that occurring in the octameric Al complexes $[HAl(NHPr^i)]_8$ [37] and $[MeAl(NMe)]_8$ [38]. The 16-membered polyhedral cage of **13** can be regarded as being made up of two interlocked 'broken cubes' fragments $[Sb_2(NCy)_2Li_2(NCy)_2]$. The geometric constraints imposed by the rhombic Sb_2N_2 rings are responsible for the inability for each $[Sb_2(NCy)_2Li_2(NCy)_2]$ half of **13** (the anticipated structure of the product) to

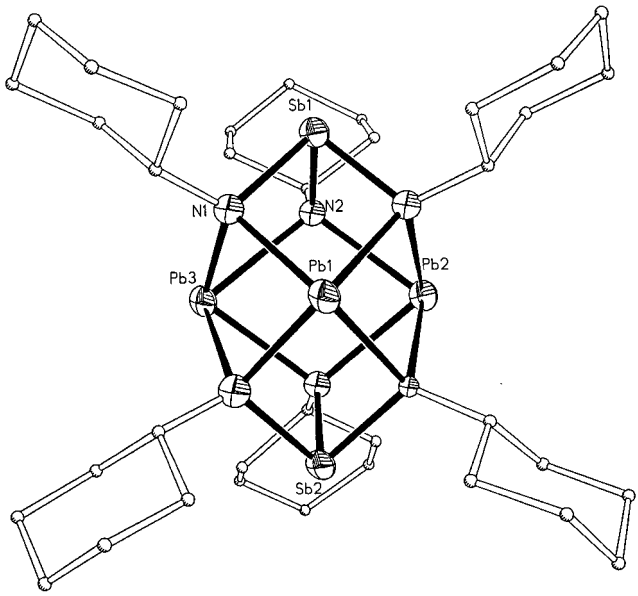

Fig. 11. The crystal structure of $\{[Sb(NCy)_3]_2Pb_3\}$ (**11**).

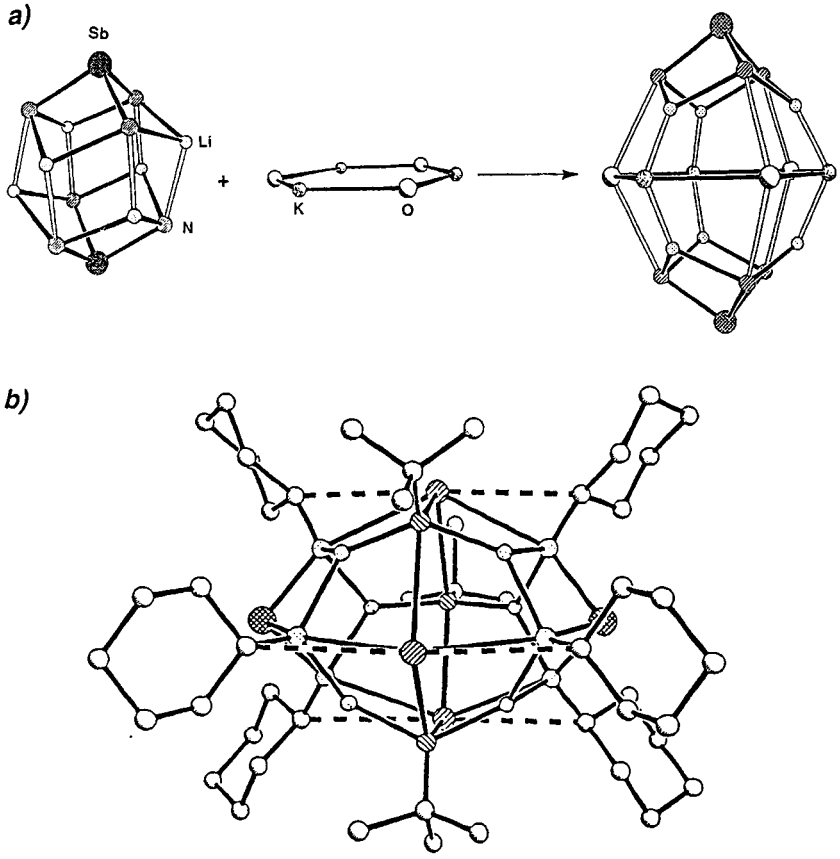

Fig. 12. (a) Schematic representation of the cage expansion of $\{[Sb(NCy)_3]_2Li_6 \cdot 2HNMe_2\}$ (**9**) with $[KOBu^t]$ and (b) structure of **12**.

close into separate cubane units. Instead, the association of two broken cubes, by the formation of Li–N bonds, appears to be preferred. This situation can be compared to that observed in the mixed Na/Li complex $[Bu^t(Ph)C = N]_6Li_4Na_2$ [39] which, in the absence of such constraints, forms a typical 'triple-stack' structure [4,5].

The similarl reaction between the potent base $[Bi(NMe_2)_3]$ and Bu^tNH_2 yields the dimer $[Me_2NBi(\mu\text{-}NBu^t)]_2$ which gives $[Bi_2(NBu^t)_4]Li_2 \cdot 2THF$ (**14**) upon reaction with $[Bu^tNHLi]_n$ in THF [40]. In this complex lithium solvation by THF prevents the formation of a structure akin to **13** and the cubane constituents of this arrangement are isolated (Fig. 14). The complex is a rare example of an imido compound of Bi (the first example was recently reported by Noltemeyer et al. [41]). Variable-temperature ^7Li NMR investigations and cryoscopic molecular mass measurements show that **14** remains as an *intact* cube in solution, whereas **13** is

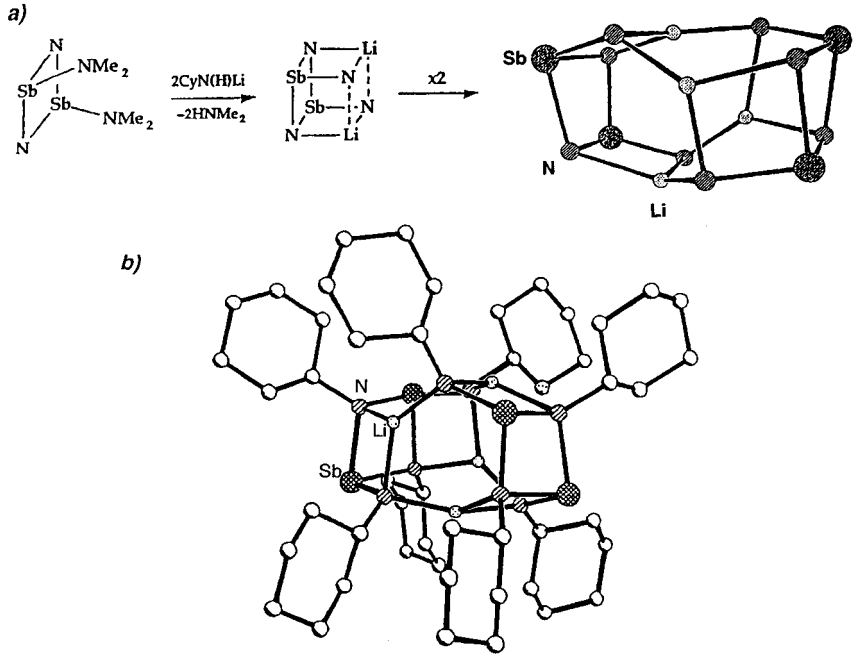

Fig. 13. (a) Schematic representation of the construction of the core of $[Sb_2(NCy)_4]_2Li_4$ (**13**) from two interlocked broken cubes and (b) structure of the complex.

involved in a dissociative equilibrium between the interlocked cube structure and the cubane units, i.e. $\{[Sb_2(NCy)_4Li_2]_2\} \rightleftarrows 2\{[Sb_2(NCy)_4]Li_2\}$.

The structure of the Na complex $\{[Sb_2(NCy)_4]_2Na_4\}$ (**15**) [42], prepared by the reaction of $[MeNSb(\mu\text{-NCy})]_2$ with [CyNHNa], has similar features as are observed in **13**. However, despite the similarity with **13** in terms of its composition, the accommodation of the larger alkali metal cations by the $[Sb_2(NCy)_4]^{2-}$ dianions in **15** has a profound effect of the geometry of the cage. The most obvious result is the adoption of a planar, rhombic Na_4 arrangement at the centre of the cage rather than the tetrahedral pattern that is present in **13**. As a consequence of the greater ionic radius of Na^+ and of the correspondingly longer alkali metal–N bonds, the $\{[Sb_2(NCy)_4]Na_2\}$ halves of the molecule no longer resemble cubane fragments. The strain induced by the complexation of the larger cations results in greater puckering in the $[Sb(\mu\text{-NCy})]_2$ rings of the $[Sb_2(NCy)_4]^{2-}$ dianions, which are splayed open in order to engage the Na^+ cations using their μ-NCy and pendent NCy groups. The major advantage of this more open arrangement is that the Na^+ cations ultimately obtain a greater coordination number than is observed for the Li^+ cations of **13**, with each being bonded to a μ-NCy and pendent NCy group of the $[Sb_2(NCy)_4]^{2-}$ dianions in the molecule. The molecular arrangement of **15** can be rationalised in terms of the compromise between the bonding demands of the $[Sb_2(NCy)_4]^{2-}$ dianions and the coordination requirements of the

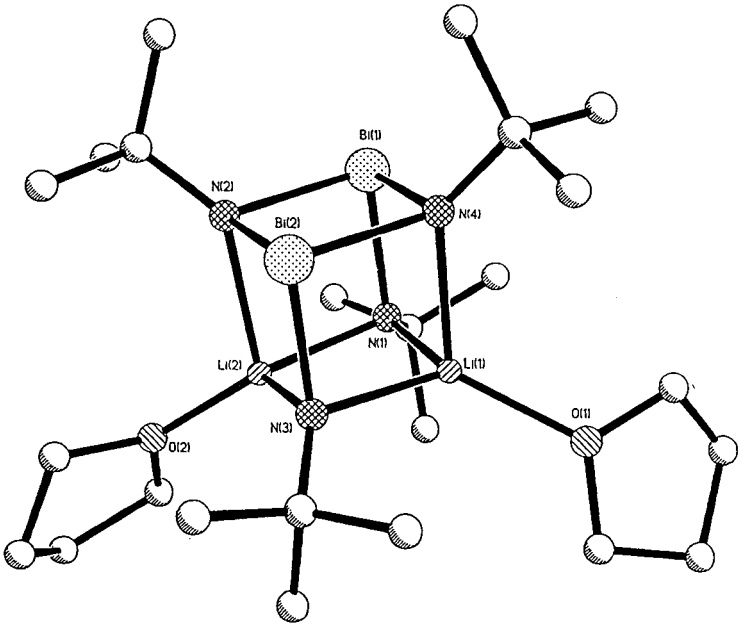

Fig. 14. Crystal structure of $[Bi_2(NBu^t)_4]Li_2 \cdot 2THF$ (**14**).

Na^+ cations. Like the trianion systems discussed in the previous section, the more rigid bonding demands of the $[Sb_2(NCy)_4]^{2-}$ dianion units clearly dominate this balance, as can be seen from the similarity of the bond lengths and angles observed in the $[Sb_2(NCy)_4]^{2-}$ dianions of **13** and **15** and from the large rearrangement in the amido–alkali metal core geometry. The considerable strain within this arrangement is particularly apparent in the extremely irregular, squared-based pyramidal coordination geometries of the Na^+ cations.

In a similar way to the alkali metal complexes containing $[Sb(NR)_3]^{3-}$ trianions, alkali metal complexes like **13**–**15** are sources of $[E_2(NR)_4]^{2-}$ dianion ligands (type *II*, Fig. 5) and can be used to build other heterometallic cages. The transmetallation reactions of **13** with CuCl and $AgCH_3CO_2$ (1:4 equivalents) yield $[Sb_2(NCy)_4]_2Cu_4$ (**16**) [34,43] and $[Sb_2(NCy)_4]_2Ag_4$ (**17**) [34], with little or no reduction of Sb(III) into the metal [Eq. (6)]. The crystal structures of **16** (Fig. 15) and **17** show them to be polyhedral cages in which two terminal $[Sb_2(NCy)_4]^{2-}$ ligands stabilise central square planar Cu_4 and Ag_4 cores. The M_4 cores in both complexes are very similar, with the terminal CyN– groups of each of the $[Sb_2(NCy)_4]^{2-}$ ligands forming M-(μ-N)-M bridges at opposite edges of the M_4 units and with longer metal–N interactions being made with the bridging imido groups of the Sb dianions. This mode of metal coordination is identical to that found in the Na^+ complex **15**, in which a similar planar, rhombic Na_4 core is present. Unlike the Na complex in which Na ⋯ Na bonding is highly unlikely [4,5],

$$[\{Sb_2(NCy)_4\}_2Li_4 + 4MX \longrightarrow [\{Sb_2(NCy)_4\}_2M_4 + 4LiX \quad \ldots(6)$$

MX= CuCl, **16**; $AgCH_3CO_2$, **17**

closed-shell metal ⋯ metal interactions are a well-established feature in Cu(I) and Ag(I) complexes and these may play a role in stabilising the M_4 cores of **16** and **17**. The Cu ⋯ Cu distances in the core of **16** (average 2.57 Å), although somewhat longer than those observed in $[CuCH_2SiMe_3]_4$ (2.42 Å) [44], are almost identical to those present in Cu metal (2.56 Å) [45,46]. The Ag ⋯ Ag distances in **17** (average 2.81 Å) are similar to those found in the structures of a number of Ag_4 complexes (approx. 3.0–3.1 Å) [47].

2.2.3. Polyimido-antimonates containing $\{[(R^1R^2N)Sb(NCy)_2]_2Sb\}^-$ monoanions

The synthesis of the first monoanionic Sb(III) imido species, $\{[(Me_2N)Sb(\mu\text{-}NCy)]_2Sb\}Li$ (**18**), involved the metallation of Sb(III) anion of $Sb[N(H)Cy]_4Li$ with $[Sb(NMe_2)_3]$ (1:2 equivalents respectively) [Eq. (7)] [18,42]. The 10e Sb(III) centre of the $Sb[N(H)Cy]_4^-$ anion becomes the central Sb present in the *spiro* structure of the $\{[(Me_2N)Sb(\mu\text{-}NCy)]_2Sb\}^-$ anion formed (type *I*, Fig. 5). The low-temperature X-ray study of **18** shows it to have an $[Sb_3N_6Li]$ 'deck-chair' core of two 'back-to-back' distorted cubic fragments sharing a common face (Fig. 16). Four μ-NCy ligands link the central four coordinate Sb centre to the two terminal three coordinate Sb atoms. Two of these μ-NCy bridges and the terminal Sb-attached NMe_2 groups are coordinated to a Li^+ cation. Complex **18** is therefore an ion-pair of the trinuclear imido-antimony anion $\{[Me_2NSb(\mu\text{-}NCy)_2]^2Sb\}^-$ and Li^+.

Unlike the stepwise process used in the preparation of **18**, the preparation of the monoanion complexes $\{[(CyNH)Sb(\mu\text{-}NR)]_2Sb\}K$ (**19**) and $\{[(CyNH)Sb(\mu\text{-}NR)]_2Sb\}Rb$ (**20**) were achieved directly by the simple *insitu* reactions of $[Sb(NMe_2)_3]$ (three equivalents) with a mixture of $CyNH_2$ (six equivalents) and [CyNHM] (M = K, Rb) (one equivalent) [47]. This route provides the cleanest and without doubt the best route to the related $\{[(CyNH)Sb(\mu\text{-}NCy)]_2Sb\}^-$ monoanion. Although it is not clear how the *spiro* Sb–N framework of the monoanion comes about from this reaction, Norman et al. [48] have recently shown that the reaction of $SbCl_3$ with [RNHLi] (1:3 equivalents) gives the imido Sb(III) dimer $[(RNH)Sb(\mu\text{-}NR)]_2$. The related complex $[(CyNH)Sb(\mu\text{-}NCy)]_2$, generated from the reaction of $[(Me_2N)Sb(\mu\text{-}NCy)]_2$ with excess $CyNH_2$, is a possible intermediate in the formation of the $\{[(CyNH)Sb(\mu\text{-}NCy)]_2Sb\}^-$ anion, which may arise from equilibration between $[(CyNH)Sb(\mu\text{-}NCy)]_2$ and $[Sb_2(NCy)_4]^{2-}$. However, it should be noted that repeated attempts to prepare various neutral dimers $[(CyNH)Sb(\mu\text{-}NR)]_2$, by the reaction of $[(Me_2N)Sb(\mu\text{-}NR)]_2$ (R = Cy, 2-$MeOC_6H_4$) with RNH_2, have so far failed owing to the surprisingly low reactivity of the terminal Me_2N groups with primary amines (only the unreacted species $[(Me_2N)Sb(\mu\text{-}NR)]_2$ being isolated).

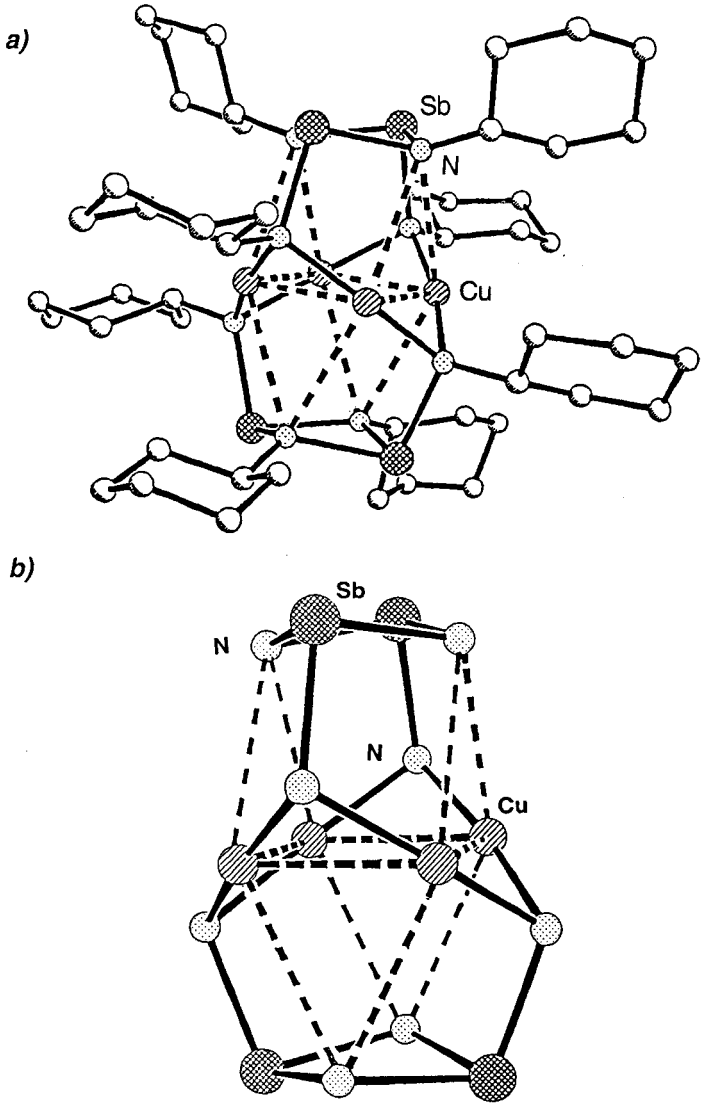

Fig. 15. (a) Crystal structure of $[Sb_2(NCy)_4]_2Cu_4$ (**16**) and (b) the core of the molecule.

The molecular structures of $\{[(Me_2N)Sb(\mu\text{-}NCy)]_2Sb\}Li$ (**18**) (Fig. 16), $\{[(CyNH)Sb(\mu\text{-}NR)]_2Sb\}K \cdot 2thf$ (**19**) and $\{[(CyNH)Sb(\mu\text{-}NR)]_2Sb\}Rb \cdot 2thf$ (**20**) (Fig. 17) both contain similar imido Sb(III) monoanion ligands which consist of two fused Sb_2N_2 rings sharing a central four-coordinate, (10e) square-based pyramidal Sb centre.

The alkali metal cations are coordinated in a similar way in **18**–**20**, by the terminal amido ligands of the Sb(III) monoanions and by two of the μ-NCy imido

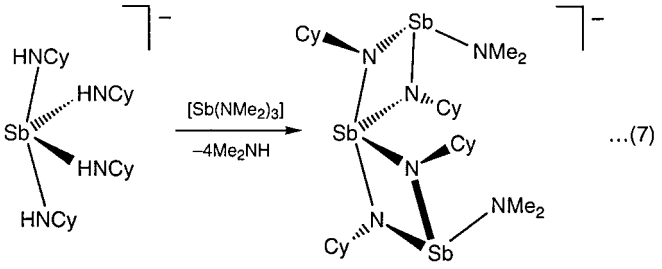

...(7)

groups within the $[Sb_3N_4]$ cores. In the K and Rb complexes the alkali metal cations are additionally coordinated by two thf molecules. Despite the obvious differences in the steric requirements of the terminal NMe_2 and NHCy substituents present in **18**, **19** and **20** and the differing coordination numbers and ionic

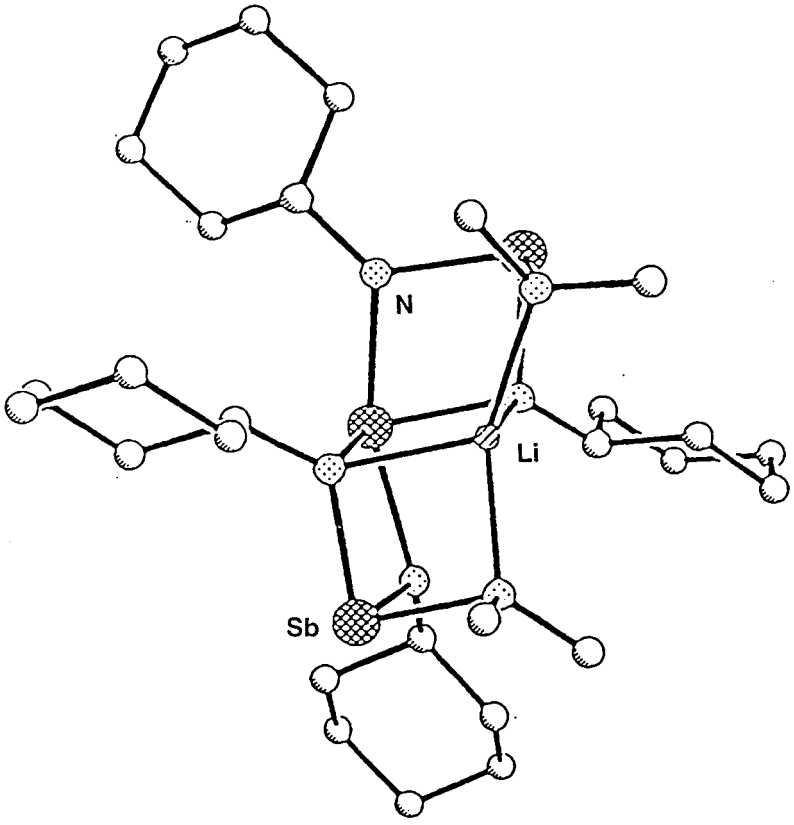

Fig. 16. Crystal structure of {[$(Me_2N)Sb(\mu$-NCy)]$_2$Sb}Li (**18**).

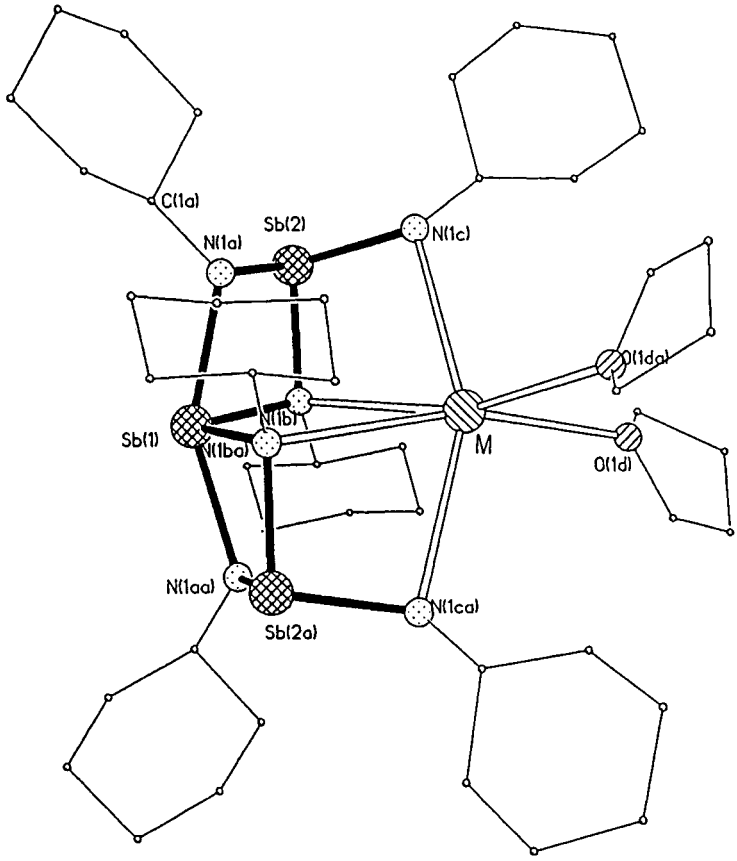

Fig. 17. Crystal structure of $\{[(CyNH)Sb(\mu\text{-}NR)]_2Sb\}M \cdot 2thf$ [M = K (**19**), Rb (**20**)].

radii of the alkali metal cations in these species, the geometries of their imido Sb(III) anions are extremely similar. The pattern of (short, medium and long) Sb–N bond lengths and N–Sb–N angles within these units largely reflects the electronic and bonding demands of the Sb(III) centres. The longest Sb–N bonds occur at the axial positions of the four coordinate (10e) Sb(III) centres, with Sb–N bonds of intermediate lengths being found at the equatorial positions, and the shortest Sb–N bonds occurring at the terminal, three-coordinate (8e) Sb(III) centres. The slightly asymmetrical structure of the $\{[(Me_2N)Sb(\mu\text{-}NCy)]_2Sb\}^-$ anion of **18** presumably results from the strain induced by the accommodation of the smaller Li^+ cation into the cage arrangement and from the presence of stronger alkali metal–N bonds which can compete more effectively for the electron density on the NCy groups. In this connection, the greatest difference in the geometries of the imido Sb(III) anions of **18**–**20** occurs in the N–Sb–N angle between the equatorial NCy groups of the four-coordinate Sb centre. The expan-

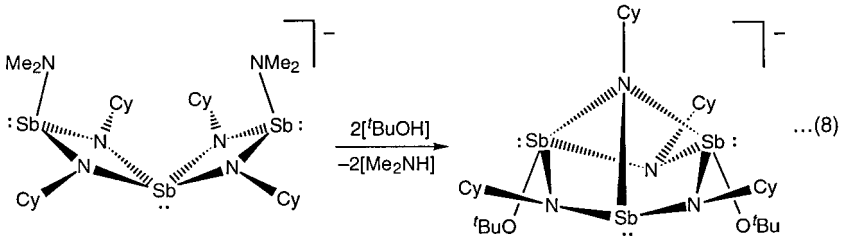

...(8)

sion of this angle from **18** to **19** and **20** correlates with the increased size of the coordinated alkali metal cations, which are chelated by the equatorial NCy groups, and presumably results in a reduction in strain within the more symmetrical structures of **19** and **20**.

The terminal NMe_2 groups of the $\{[(Me_2N)Sb(\mu\text{-}NCy)_2]_2Sb\}^-$ anion are reactive towards organic acids. In the 1:2 reaction of $\{[(Me_2N)Sb(\mu\text{-}NCy)_2]_2Sb\}K$ with $CyNH_2$ in toluene, the *spiro* structure of the monoanion is retained [49]. However, the reaction $\{[(Me_2N)Sb(\mu\text{-}NCy)_2]_2Sb\}K$ with $[Bu^tOH]$ (1:2 equivalents) is accompanied by structural isomerism of the anion into a *nido* cage arrangement [Eq. (8)]. The product of this reaction is $\{[(Bu^tO)_2Sb_3(\mu\text{-}NCy)_3(\mu_3\text{-}NCy)]K \cdot (\eta^6\text{-}C_6H_5CH_3)\}$ (**21**) [49]. It appears this rearrangement is a result of the increased Lewis acidity of the O-attached metal centres, with the *nido* structure of **21** maximising their coordination numbers. Although this same effect can also be seen to underlie the coordination of Me_2NH to Sb(III) in $[SbCl(Me_2NH)(\mu\text{-}NBu^t)]_2$ (**2**) [17] [during the reaction of $[(Me_2N)_2ClSb]$ with Bu^tNH_2 (see Section 2.1)] and the aggregation of $[Cl_3SbNMe]_4$ into a cubane (as opposed to a dimer) structure [50], the formation of **21** provides the first example of the intramolecular structure directing influence of the electronegativity of ligands on cage geometry within this type of p block metal system.

In **21**, the K^+ is coordinated at the open Sb_3N_3 face of the *nido* $[(Bu^tO)_2Sb_3(\mu\text{-}NCy)_3(\mu_3\text{-}NCy)]^-$ anion and by a π-bonded toluene molecule (Fig. 18). The anion of **21** is composed of three Sb(III) centres which are linked together in the equator by three μ-NCy groups and capped by a μ_3-NCy group. Additionally, two of the Sb atoms are complexed by terminal OBu^t groups, resulting in a 10e pseudo trigonal bipyramidal geometry for these centres and with the other Sb atom having an 8e pyramidal geometry. Although there are obvious differences between the electron precise bonding in the *nido* complex **21** and structurally similar electron deficient borane ligands, the localised $[Sb(\mu\text{-}NCy)]_3$ face is isoelectronic with the open C_2B_3 face of 2,4-$[R_2C_2B_4H_4]_2^-$ [51], suggesting that the *nido* $[(Bu^tO)_2Sb_3(\mu\text{-}NCy)_3(\mu_3\text{-}NCy)]^-$ anion may perform an analogous structural role as a building block in metal complexes [52,53].

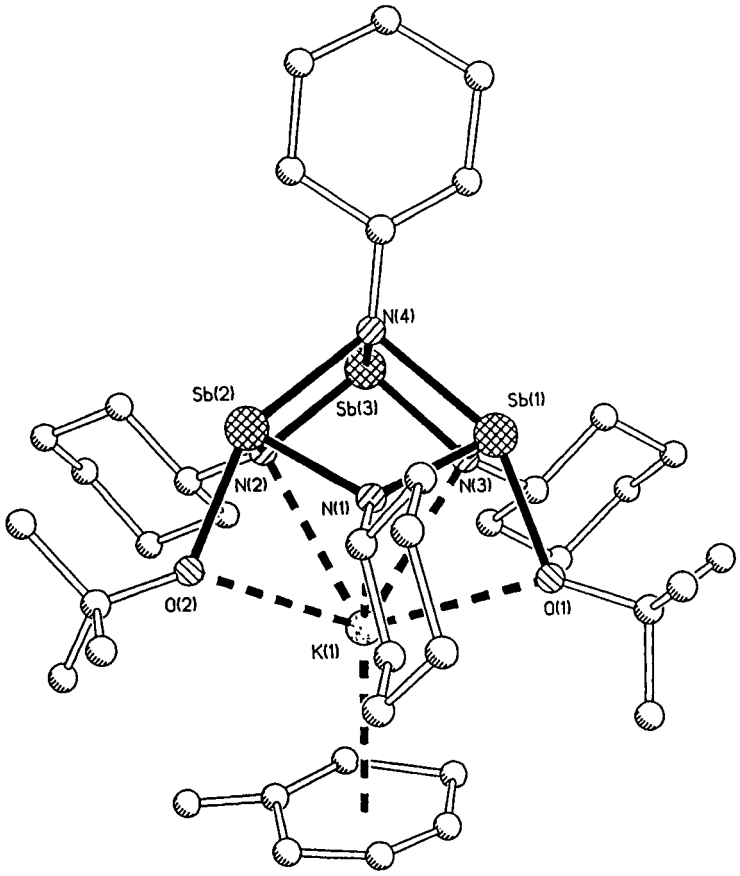

Fig. 18. Crystal structure of $\{[(Bu^tO)_2Sb_3(\mu\text{-NCy})_3(\mu_3\text{-NCy})]K\cdot(\eta^6\text{-}C_6H_5CH_3)\}$ (**21**).

3. Group 14 systems

3.1. Reactions of [Sn(NMe$_2$)$_2$] with primary amines

The previous studies had shown that dimethyl amido Group 15 reagents are highly useful in preparing imido and phosphinidene complexes. Furthermore, these reagents provide a simple route to heterometallic systems containing novel anionic ligand arrangements. In further studies we wanted to extend the synthetic methodology of step-wise metallation of primary amines and phosphines to Group 14 systems. As a prelude to more extensive investigations of the formation of anionic Group 14 imido and phosphinidene ligands, the reactivity of $[Sn(NMe_2)_2]$ [12] with primary amines was examined.

The reactions of sterically undemanding aliphatic primary amines (RNH_2) provides an efficient route to the cubanes $[SnNR]_4$ (R = Cy (**22**), 2-$NCH_2C_5H_4$

$$4[Sn(NMe_2)_2] + 4RNH_2 \longrightarrow [Sn(NR)]_4 + 8Me_2NH \quad ...(9)$$

(**23**) [54], Bu^t (**24**) [55] [Eq. (9)]. Although several imido-Sn(II) cubanes have been prepared by a variety of routes [56–59], the use of $[Sn(NMe_2)_2]$ allows the general and facile syntheses of these species. For example, Veith has shown that the cubanes $[ENR]_4$ (E = Ge, Sn, Pb; R = Bu^t, Pr^i, $NNMe_2$) can be prepared at room temperature or above by the reactions of $[Me_2Si(\mu\text{-}NBu^t)Sn]$ with primary amines and hydrazines [56–58]. In addition, Power has employed that the reactions of $\{E[N(SiMe_3)_2]_2\}$ (E = Sn, Pb) with suitable primary aromatic amines (in the melts at 50–60°C) or borylamines (in hexane at reflux) in the preparation of Sn(II) and Pb(II) imido cubanes [59]. The particular advantage of the use of $[Sn(NMe_2)_2]$ over existing routes is that Sn(II) imido cubanes can be prepared at very low temperatures ($\leq$ 20°C) and using relatively non-acidic primary amines (in which there is no conjugative stabilisation of the imido dianions). Thus, thermally unstable species [such as the Sn(II) cubane **23** (decomp. approx. 30°C)] are accessible using this route.

The structure of **23** is of some interest, the complex being the only example of a Group 14 cubane in which accessible donor functionality is present. Although the angles within the Sn_4N_4 core of **23** are similar to those in **22** and **24**, the Sn–N bond lengths are considerably more irregular as a result of weak intramolecular pyridyl-N $\cdots$ Sn interactions. The interaction of three pyridyl groups with separate Sn centres of the core is subtly reflected in the packing of the molecules in the lattice. The cubane molecules of **23** are arranged in loose strands which are associated by weak intermolecular Sn $\cdots$ Sn interactions, with the shortest metal–metal interaction occurring between the least coordinated tin centres of the neighbouring molecules (Fig. 19). Although loose Sn $\cdots$ Sn interactions have been observed in $[Sn(NNMe_2)]_4$ [56,57], the pattern of association in **23** illustrates that such interactions can be modified by the effects of intramolecular donation within the Sn_4N_4 units.

The reactions of $[Sn(NMe_2)_2]$ with sterically demanding aromatic amines do not give the cubanes $[SnNR]_4$. Instead, the heteroleptic imido/amido tin(II) complexes $\{Sn(NR)_2[Sn(\mu\text{-}NMe_2)]_2\}$ [R = 2,6-$Pr^i_2C_6H_3$ (Dipp) (**25**), 2,4,6-$Me_3C_6H_2$ (Mes) (**26**) (Fig. 20)] are formed [60]. These species are model intermediates in the formation of Group 14 trimeric rings, $[ENR]_3$, and cubanes $[ENR]_4$ (E = Ge, Sn, Pb).

The initial stage in the formation of cubanes appears to be the single deprotonation of $[RNH_2]$ by $[Sn(NMe_2)_2]$ [Eq. (10)]. The intermediate produced, most likely the dimer $[(RNH)Sn(\mu\text{-}NMe_2)]_2$ in which the least sterically bulky NMe_2 groups are bridging, then undergoes further metallation with $[Sn(NMe_2)_2]$ to give species akin to **25** and **26**. Only with more extreme conditions do the 1:1 reactions of $[Sn(NMe_2)_2]$ with $[RNH_2]$ proceed to the cubanes $[Sn(NR)]_4$ (e.g. 2.5 days at reflux in toluene for **26**). The most plausible intermediate involved for the conversion of

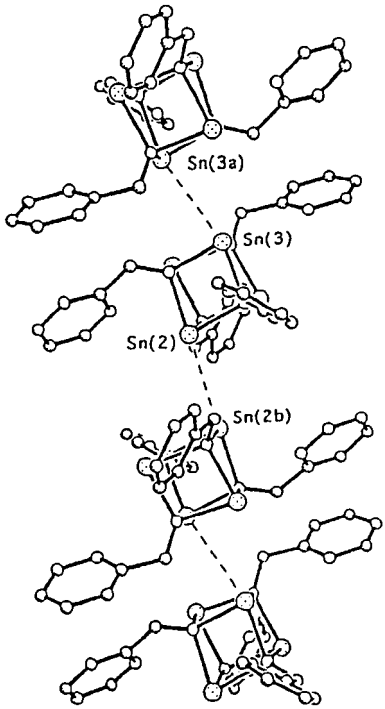

Fig. 19. Intermolecular packing of complex $[Sn(2\text{-}NCH_2C_5H_4N)]_4$ (**23**) via Sn ⋯ Sn interactions.

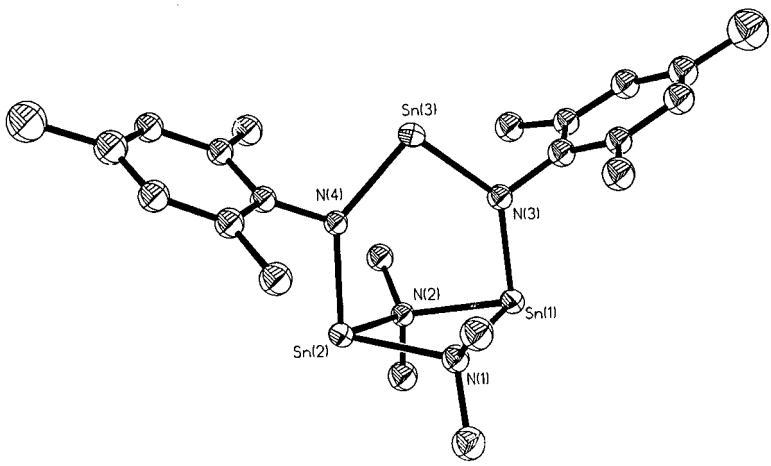

Fig. 20. Molecular structure of $\{Sn(NMes)_2[Sn(\mu\text{-}NMe_2)]_2\}$ (**26**).

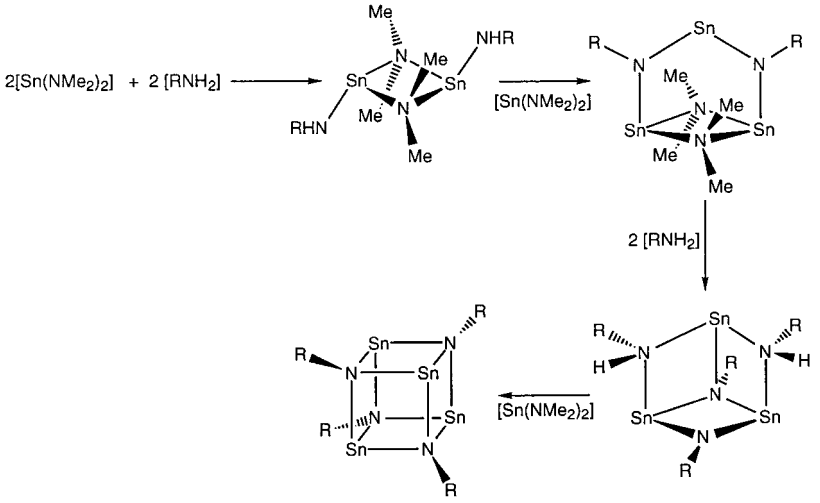

$\{Sn(NR)_2[Sn(\mu\text{-}NMe_2)]_2\}$ into the cubanes is $\{[Sn(\mu\text{-}NR)]_2[Sn(NHR)_2]\}$ (structurally identical to the previously characterised complex $\{[Sn(\mu\text{-}NBu^t)]_2[Sn(NHBu^t)_2]\}$ [61,62]). It is interesting to note that whereas the cubane $[Sn(NDipp)]_4$ is formed by the reaction of $\{Sn[N(SiMe_3)_2]_2\}$ with $[DippNH_2]$, the analogous reaction with $\{Ge[N(SiMe_3)_2]_2\}$ produces the trimer $[Ge(NDipp)]_3$ [59,63]. This can be explained by the reaction of an analogous intermediate to **25** and **26** [bearing $N(SiMe_3)_2$ groups instead of NMe_2] with $[DippNH_2]$, terminating the reaction sequence at the trimer. Thus, the isolation of **25** and **26** provides the first indication that the formation of Group 14 imido cubanes from metallation reactions of primary amines with various Group 14 reagents may proceed via a common sequence of reactions involving step-wise metallation of imido/amido intermediates. This is in contrast to the established mechanism of formation of $[SnNBu^t]_4$ from the thermolysis of $[(Me_2Si)(NBu^t)_3Sn_2]$, in which oligomerisation of the 'stannylene' [:Sn-NBu^t] is involved [64].

An unprecedented feature of **25** and **26** is the coordination of the tin atoms within the $Sn(NR)_2$ units exclusively by only two imido centres (the lowest coordination number for Sn(II) centres in imido complexes). Although the steric bulk of the organic substituents in **25** precludes intermolecular Sn ⋯ Sn interactions from occurring, in **26** intermolecular interactions occur between one of the Sn(II) centres of the $[Sn(\mu\text{-}NMe_2)]_2$ (formally 8e donor) unit of one of the molecules and the $Sn(NMes)_2$ (formally 6e acceptor) unit of the neighbouring molecule. The result being the formation of loosely-linked hexameric rings (Fig. 21) which are connected by Sn ⋯ Sn (donor/acceptor and donor/donor) contacts into a network of fused four-, six- and eight-membered rings.

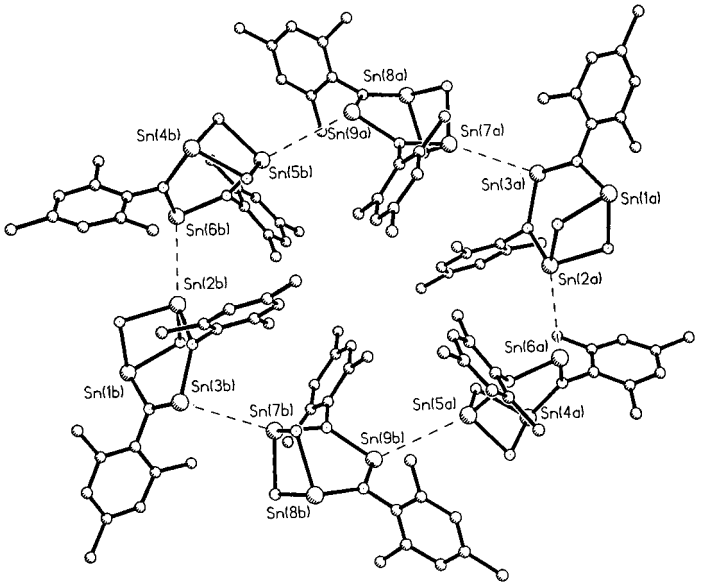

Fig. 21. Loosely-linked hexameric rings of $\{Sn(NMes)_2[Sn(\mu\text{-}NMe_2)]_2\}$ (**26**).

3.2. Heterometallic arrangements containing Sn(II) imido and phosphinidene anions

The high reactivity of $[Sn(NMe_2)_2]$ primary amines gave good promise that metallation of primary amido lithium complexes would, in a similar way to the Group 15 systems, generate imido Sn(II) anions. However, it soon became apparent that this synthetic approach would not be successful for Group 14. In all cases the 2:1 reactions of [RNHLi] with $[Sn(NMe_2)_2]$ give the cubanes $[SnNR]_4$ rather than complexes of the type $[Sn(NR)_2Li_2]_n$ which were sought. It became obvious then that new synthetic strategies which avoided the apparently overwhelming thermodynamic preference for the cubanes would be necessary in the preparation of imido Sn(II) anion arrangements.

One potential strategy which proved successful is employing the mixed amido/imido complexes $\{Sn(NR)_2[Sn(\mu\text{-}NMe_2)]_2\}$ (**25** and **26**) as polynuclear reagents. These species can be seen, on a synthetic level, as analogous to the reactive amido/imido, dimers $[Me_2NSb(\mu\text{-}NR)]_2$ (see Section 2.1). However, the reaction of $\{Sn(NMes)_2[Sn(\mu\text{-}NMe_2)]_2\}$ (**26**) with [LiN(H)ma] [ma = (2-MeO)C_6H_4] (1:2 equivalents) follows an unexpected pathway in which the elimination of $[Sn(NMe_2)_2]$, rather than deprotonation of the primary amido lithium, gives rise to the heterobimetallic ladder complex $\{[MesNHSn(\mu\text{-}Nma)]_2(Li \cdot 2thf)_2\}$ (**27**) [Eq. (11)] [65]. A crystallographic study shows it to be formed from the association of the imido Sn(II) dianion $[MesNHSn(\mu\text{-}Nma]_2^{2-}$ with two THF-solvated Li^+ cations (Fig. 22). Alternatively, the structure can be regarded as composed of a central imido Sn(II) dimer which is solvated by two primary amido lithium

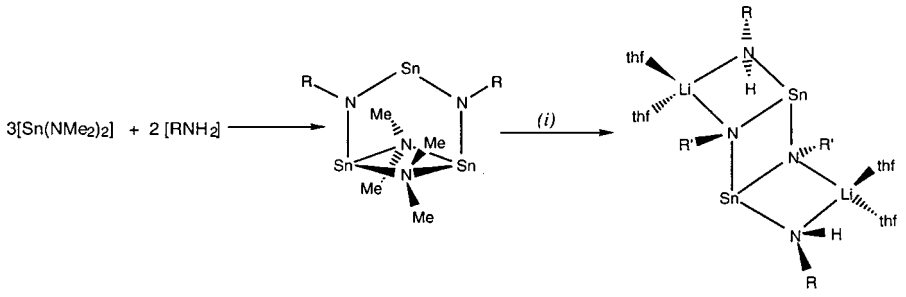

monomers. Calculational studies of **27** illustrate that the preference for the ladder arrangement containing a central Sn_2N_2 core (e.g. vs. a THF solvated $\{(Sn_2N_2)[(HN)_2Li_2]\}$ cubane) is largely dictated by solvation of Li^+. It is interesting to compare the arrangement found in **27** with the Bi(III) imido complex $[Bi_2(NBu^t)_4]Li_2 \cdot 2THF$ (**14**) (Figure 14) [40], where even in the presence of THF solvation of Li^+ the structure adopted is that of a cubane.

Although reactions of $[Sn(NMe_2)_2]$ with primary amido lithium complexes have so far proved ineffective in the synthesis of imido Sn(II) anions, the facile synthesis of Group 14 cubanes (noted above in Section 3.1) furnishes another approach to

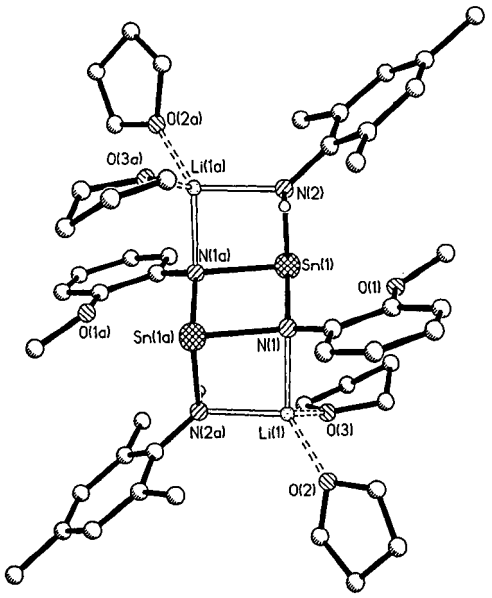

Fig. 22. The crystal structure of heterobimetallic ladder $\{[MesNHSn(\mu\text{-Nma})]_2(Li \cdot 2thf)_2\}$ (**27**).

$$[SnN^tBu]_4 + 4Ph_3CSH \longrightarrow 2[(Ph_3CS)Sn(\mu\text{-}HN^tBu)]_2 \quad \ldots(12)$$

(28)

$$[SnN^tBu]_4 + 3[C_{10}H_7NHLi] \longrightarrow [Li(THF)_4]^+[^tBuN(C_{10}H_7N)_3Sn_3Li.THF]^- \quad \textbf{(29)}$$

$$+ [Sn(\mu\text{-}NH^tBu)_3Li] \quad \ldots(13)$$

these species. The simple acid/base reaction of $[SnNBu^t]_4$ (**24**) with $[Ph_3CSH]$ (1:4 equivalents) illustrates that the imido Sn(II) cubanes themselves can be employed as the metallating reagents. The product of this reaction, the dimer $[(Ph_3CS)Sn(\mu\text{-}NHBu^t)]_2$ (**28**) [55], results from the symmetrical cleavage of the imido Sn(II) cubane [Eq. (12)].

If sufficiently acidic primary amido or phosphido lithium precursors are used in this reaction then the acid/base fragmentation of the cubane leads to the desired imido and phosphinidene anions. The reaction of $[C_{10}H_7NHLi]$ ($C_{10}H_7$ = 1-naphthyl) with the cubane **24** (4:1) gives the complex $[Li(THF)_4]^+[Bu^tN(C_{10}H_7N)_3Sn_3Li \cdot THF]^-$ (**29**) (Fig. 23) [66]. The structure of the heterometallic polyimido anion of **29**, $[Bu^tN(C_{10}H_7N)_3Sn_3Li \cdot THF]^-$, resembles a Sn_4N_4 cube in which one Sn is substituted by a Li^+ cation. This anion arises from the association of the tripodal polyimido Sn(II) dianion $[(Bu^tN)(C_{10}H_7N)_3Sn_3]^{2-}$ with a thf solvated Li^+ cation. Although the mechanism of the reaction involved in the formation of **29** in unclear, the product appears to result from the formal extrusion of $[Sn(\mu\text{-}HNBu^t)_3Li]$ [Eq. (13)].

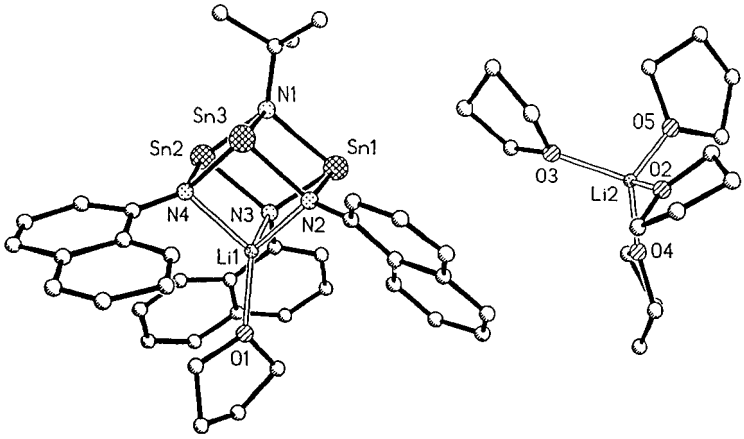

Fig. 23. The crystal structure of $[Li(THF)_4]^+[Bu^tN(C_{10}H_7N)_3Sn_3Li \cdot THF]^-$ (**29**).

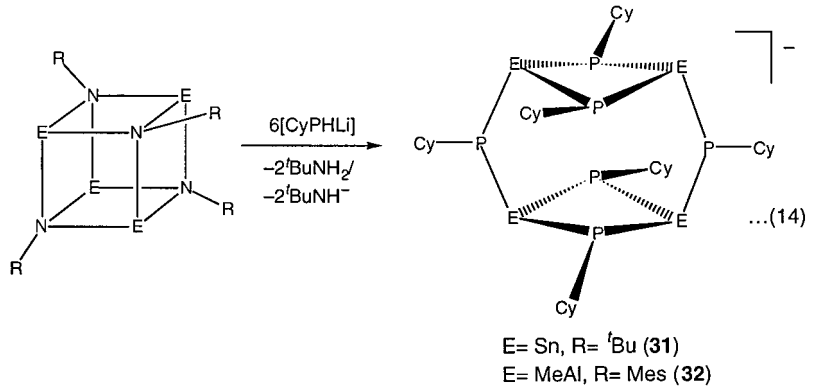

The acid/base reactions of the cubanes $[SnNBu^t]_4$ (**24**) or $[MeAlNMes]_4$ (**30**) [67] with [CyPHLi] (1:6 equivalents) yield the phosphinidene cage complexes $\{[Sn(\mu\text{-}PCy)]_2(\mu\text{-}PCy)\}_2 \cdot Li_4 \cdot 4thf$ (**31**) [66] (Fig. 24) and $\{[(AlMe)(\mu\text{-}PCy)]_2(\mu\text{-}PCy)\}_2 \cdot Li_4 \cdot 4thf$ (**32**) [Eq. (14)] [68]. Both complexes are composed of similar 14-membered $[Sn_4P_6Li_4]$ and $[Al_4P_6Li_4]$ polyhedral cores. These structural arrangements come about by the association of metallacyclic $\{[Sn(\mu\text{-}PCy)]_2(\mu\text{-}PCy)\}_2^{4-}$ and $\{[(AlMe)(\mu\text{-}PCy)]_2(\mu\text{-}PCy)\}_2^{4-}$ tetraanions with four THF-solvated Li^+ cations at the centres of the cages. Complexes **31** and **32** are rare examples of structurally characterised Sn(II) [69] and Group 13 [70–75] phosphinidine complexes. Apart

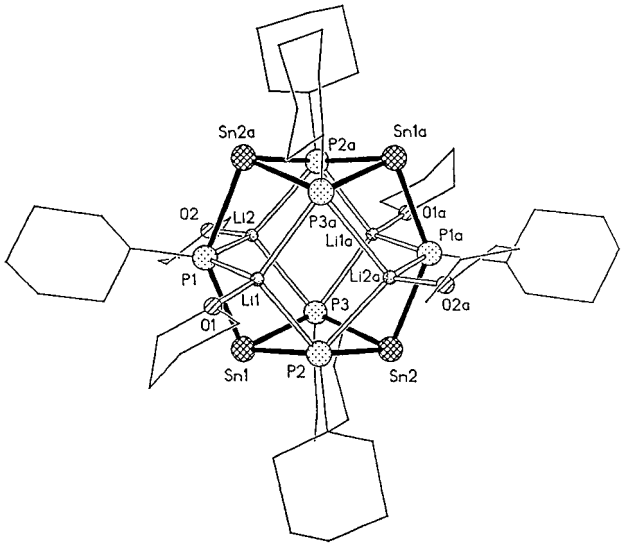

Fig. 24. The crystal structure of $\{[Sn(\mu\text{-}PCy)]_2(\mu\text{-}PCy)\}_2 \cdot Li_4 \cdot 4thf$ (**31**).

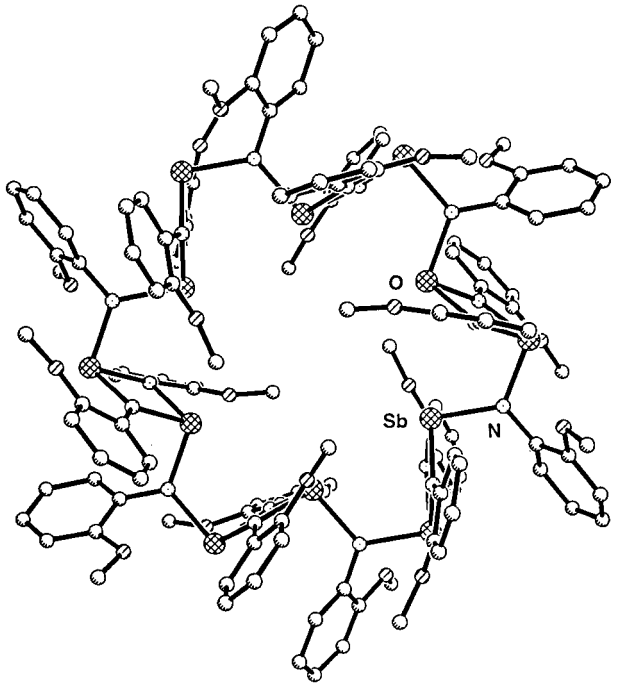

Fig. 25. The crystal structure of the metallacycle $[Sb_{12}(Nma)_{18}]$ (**34**).

from **32**, the only other example containing a Group 13 phosphinidene anion is that of $[Li(Et_2O)_2(Bu^tGa)(\mu\text{-}PBu^t)_2(GaBu^t_2)_2]$ [76]. The metallacyclic tetraanions of **31** and **32** represent entirely new metal-based ligand environments for the complexation of a range of metals.

4. Metallacyclic complexes

The discussion so far has concerned the reactions of primary amido or phosphinidene alkali metal complexes with p block metal reagents. However, a recent area of interest has concerned the reactions of other main group metal primary amido and phosphinidene complexes with dimethyl amido reagents. The nucleophilic substitution reaction of [LiN(H)ma] with Cp_2Sn gives the tris(primary amido)stannate complex $[(maNH)Sn(\mu\text{-}NHma)_2Li \cdot THF]$ (ma = 2-$MeOC_6H_4$) (**33**) [77], the $[Sn(NHma)_3]^{3-}$ anion of which contains three potentially reactive protons. In an attempt to generate a mixed-metal cage anion $[Sn(\mu\text{-}Nma)_3Sb]^-$, **33** was reacted with $[Sb(NMe_2)_3]$. However, the product of this reaction is the Sb(III) complex $[Sb_{12}(Nma)_{18}]$ (**34**) [78], composed of six Sb_2N_2 dimeric rings linked by bridging imido groups into a 24-membered metallacyclic ring (Fig. 25). This arrangement is similar to that occurring in the tetraanion complexes **31** and **32**.

The Sb_2N_2 units of **34** and the pattern of intramolecular MeO ··· Sb interactions within these are almost identical to that occurring in the dimer $[(Me_2N)Sb(\mu\text{-NMA})]_2$ (**35**) [14]. It is interesting to note, however, that the metallacyclic complex does not result from the reaction of **35** with excess $maNH_2$ and it therefore appears that the formation of **34** is fundamentally reliant on the reaction sequence. However, further studies are required in order to determine what the mechanism involved in the formation of **34** is.

The orientation of the dimeric Sb_2N_2 moieties in **34**, perpendicular to the macrocyclic core, produces an overall toroid structure. MeO ··· Sb interactions give highly distorted alternating four-coordinate and five-coordinate Sb(III) centres within the metallacyclic ring. As a result of the *inter*-dimer interactions of one of the bridging MeO groups with the four coordinate Sb centres, the associated aromatic ligands are distorted significantly out of the planes of each of Sb_2N_2 dimer moieties. The six attached methoxy ligands are directed towards the centre of the metallacycle (three above and three below the $Sb_{12}N_{18}$ ring) giving rise to an almost perfect octahedral cavity. This arrangement of the methoxy ligands presents the prospect of selective coordination of metal ions. Additionally, there is the possibility of anion complexation by the Lewis acidic Sb(III) centres.

5. Structure and reactivity of Group 16 dimethylamido complexes

A number of cage complexes $\{[E(NBu^t)_3]Li_4\}$ (E = S, Se, Te), containing tripodal $[E(NBu^t)_3]^{2-}$ dianions and having similar structural arrangement to the Sb(III) trianion complexes in Section 2.2.1 have been characterised [79–85]. These species are prepared by the addition reactions of $[Bu^tNHLi]$ to $[(Bu^tN)_2E]$. On the basis of the previous work outlined above another potential route to a variety of species containing Group 16 anion arrangements is via the dimethyl amido reagents. The preparation of $[Te(NMe_2)_2]_\infty$ (**36**) [86] in high yield from the reaction of $TeCl_4$ with $LiNMe_2$ provides a highly reactive precursor. Although the mechanism of the formation of **36** is unclear, due to the absence of disproportionation into metallic tellurium a possible mechanism is that of reductive elimination of Cl_2 from $[Te(NMe_2)_2Cl_2]$. A radical pathway similar to that proposed by Roesky et al. in the formation of $\{Te[N(SiMe_3)_2]_2\}$ involving the initial formation of $[Te(NMe_2)_4]$, is also possible [87–89]. The crystal structure of **33** reveals it to be polymeric, each of the $[Te(NMe_2)_2]$ units is linked to the next Te by weak Te ··· N interactions (Fig. 26). This structural arrangement gives each of the (12e) tellurium centres a distorted square-planar geometry, with the two lone pairs on each of the metal atoms being axially aligned. Although there have been a variety of N-bonded complexes of Te(IV) and Te(II) characterised in the solid state, very few bis(amido)tellurium(II) compounds of this type have been structurally elucidated [87–89].

The reactions of **36** with amines (e.g. Bu^tNH_2, $CyNH_2$ and $(PhCH_2)_2NH$) and phosphines (e.g. $PhPH_2$ and $CyPH_2$) occur smoothly at −78°C, giving coloured

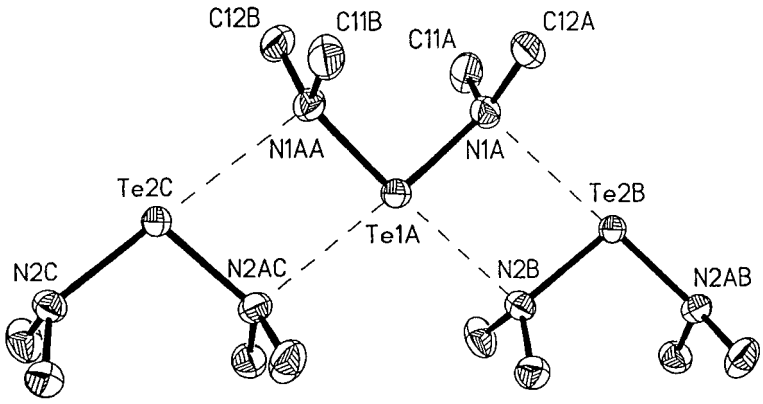

Fig. 26. The crystal structure of $[Te(NMe_2)_2]_\infty$ (**35**).

solutions and forming Me_2NH [86]. However, although these solutions are stable at low temperatures, if raised above approx. −40°C, decomposition to metallic tellurium is normally observed. Reactions with thiols (Ph_3CSH, $PHCH_2SH$ and 2-$(SH)C_5H_4N$) prove to be more successful, yielding products stable at room temperature. It appears that the presence of soft heteroatomic centres within the organic acid prevents reduction in these systems. The reaction of **36** with Ph_3CSH (1:2 equivalents respectively) produces $[Te(SCPH_3)_2]$ (**37**) [86] which is air- and moisture-stable for prolonged periods (> 30 min). The crystal structure of **37** shows it to be a simple monomer in the solid state, a result of the large steric bulk of the $SCPh_3$ groups. This is the first structurally characterised complex containing simple unfunctionalised thiolate ligands.

6. Future perspectives and closing remarks

Dimethylamido p block metal complexes are a family of reagents which provide easy access to a diverse range of metallo–organic species. In particular, their metallation reactions with primary amido and phosphido alkali metal complexes furnishes a highly versatile route to imido and phosphinidene anion systems which can be employed as ligands to a range of main group and transition metals. Future work will continue to uncover the coordination characteristics of these new ligands, particularly those of Groups 13 and 14, and expand the range of ligand functionalities available. A major focus for future studies will be the preparation of crown-like metallacycles of p block metals and their application as cation and anion selective ligands. The elucidation of the basic reaction characteristics of these reagents has laid the foundations for the targeted assembly of mixed-metal cage complexes which are potential precursors to a number of technologically important applications. Future work will also be aimed at the application of the synthetic routes developed to single-source precursors to various thin films [90].

References

[1] A.H. Cowley, R.A. Jones, Angew. Chem. 101 (1989) 1235; Angew. Chem., Int. Ed. Engl. 28 (1989) 1208.
[2] R.L. Wells, Coord. Chem. Rev. 273 (1992).
[3] M.A. Paver, C.A. Russell, D.S. Wright, Compre. Organomet. Chem., 2nd ed., in: C.E. Housecroft (Ed.), Pergamon, Ch. 11 (1995) 503 and references therein.
[4] K. Gregory, P. von R. Schleyer, R. Snaith, Adv. Inorg. Chem. 37 (1991) 47.
[5] R.E. Mulvey, Chem. Soc. Rev. 20 (1991) 167.
[6] D.R. Armstrong, W. Clegg, S.R. Drake et al., Angew. Chem., 1991; Angew. Chem., Int. Ed. Engl. 30 (1991) 1707.
[7] M.A. Paver, C.A. Russell, D.S. Wright, Angew. Chem. 107 (1995) 1677; Angew. Chem., Int. Ed. Engl. 34 (1995) 1545.
[8] A. Kiennemann, G. Levy, F. Schue, C. Tanielian, J. Organomet. Chem. 35 (1972) 143.
[9] F. Ando, T. Hayashi, K. Ohashi, J. Kotetsu, J. Nucl. Chem. 35 (1991) 2011.
[10] K. Moedritzer, Inorg. Chem. 3 (1964) 609.
[11] W. Clegg, N.A. Compton, R.J. Errington, et al., Inorg. Chem. 30 (1991) 4680.
[12] M.M. Olmstead, P.P. Power, Inorg. Chem. 30 (1984) 413.
[13] A.J. Edwards, M.A. Paver, P.R. Raithby, C.A. Russell, D.S. Wright, J. Chem. Soc., Dalton Trans. (1994) 2963.
[14] M.K. Davies, Ph.D. Thesis, University of Cambridge, 1997.
[15] N. Kuhn, O.J. Scherer, Z. Naturforsch. 34B (1979) 888.
[16] M.A. Beswick, C.N. Harmer, A.D. Hopkins, M.A. Paver, P.R. Raithby, D.S. Wright, Polyhedron, in press.
[17] A.J. Edwards, N.E. Leadbeater, M.A. Paver, P.R. Raithby, C.A. Russell, D.S. Wright, J. Chem. Soc., Dalton Trans. (1994) 1479.
[18] A.J. Edwards, M.A. Paver, P.R. Raithby, M.-A. Rennie, C.A. Russell, D.S. Wright, Angew. Chem. 106 (1994) 1334; Angew. Chem., Int. Ed. Engl. 33 (1994) 1277.
[19] D.R. Armstrong, R.E. Mulvey, G.T. Walker, D. Barr, R. Snaith, J. Chem. Soc., Dalton Trans. (1988) 617.
[20] D. Barr, W. Clegg, R.E. Mulvey, R. Snaith, J. Chem. Soc., Chem. Commun. (1984) 285.
[21] L. Zsolnai, G. Huttner, M. Dreiss, Angew. Chem. 105 (1993) 1549; Angew. Chem., Int. Ed. Engl. 32 (1993) 1439.
[22] M. Dreiss, G. Huttner, N. Knopf, H. Pritzkow, L. Zsolnai, Angew. Chem. 107 (1995) 354; Angew. Chem., Int. Ed. Eng. 34 (1995) 316.
[23] D.J. Brauer, H. Burger, G.L. Liewald, J. Wilke, J. Organomet. Chem. 269 (1985) 303.
[24] D.J. Brauer, H. Burger, G.L. Liewald, J. Organomet. Chem. 308 (1986) 119.
[25] M. Veith, A. Spaniol, J. Pohlmann, F. Gross, V. Huch, Chem. Ber. 126 (1993) 2625.
[26] N.D.R. Barnett, W. Clegg, L. Horsburgh, et al., J. Chem. Soc., Chem. Commun. (1996) 2321.
[27] M.A. Beswick, N. Choi, C.N. Harmer et al., Inorg. Chem., in press.
[28] M.A. Beswick, C.N. Harmer, A.D. Hopkins, M.A. Paver, P.R. Raithby, D.S. Wright, J. Chem. Soc., Chem. Commun., in press.
[29] M. Veith, M. Zimmer, S. Müller-Becker, Angew. Chem. 105 (1993) 1771; Angew. Chem., Int. Ed. Engl. 32 (1993) 1733.
[30] A.H. Cowley, J.G. Lasch, N.C. Norman, M. Pakulski, B.R. Whitlesey, J. Chem. Soc., Chem. Commun. (1983) 881.
[31] E. Hey-Hawkins, S. Kurz, Phosphorus, Sulphur Silicon 90 (1994) 281.
[32] P. Jutzi, U. Meyer, S. Opiela, M.M. Olmstead, P.P. Power, Organometallics 9 (1991) 1459.
[33] M.A. Beswick, C. Lopez-Casideo, M.A. Paver, et al., J. Chem. Soc., Chem. Commun. (1997) 109.
[34] M.A. Beswick, N.L. Cromhout, C.N. Harmer, et al., Inorg. Chem. 36 (1997) 1740.
[35] D. Barr, A.J. Edwards, M.A. Paver, et al., Angew. Chem. 107 (1995) 1081; Angew. Chem., Int. Ed. Engl. 34 (1995) 1012.

[36] R.A. Alton, D. Barr, A.J. Edwards, et al., J. Chem. Soc., Chem. Commun. (1994) 1481.
[37] G.D. Piero, M. Cesari, G. Perego, S. Cucinella, E. Cernia, J. Organomet. Chem. 129 (1977) 289.
[38] S. Amirkhalili, P.B. Hitchcock, J.D. Smith, J. Chem. Soc., Dalton Trans. (1979) 1206.
[39] D. Barr, W. Clegg, R.E. Mulvey, R. Snaith, J. Chem. Soc., Chem. Commun. no volume no. (1989) 57.
[40] M.A. Beswick, A.J. Edwards, J.R. Galsworthy, et al., Inorg. Chim. Acta. 9 (1996) 248.
[41] N. Noltemeyer, H.W. Roesky, H. Schmidt, U. Wirringa, Inorg. Chem. 33 (1994) 4607.
[42] M.A. Beswick, A. Bashall, C.M. Harmer et al., J. Chem. Soc., Dalton Trans., submitted.
[43] D. Barr, A.J. Edwards, S. Pullen, et al., Angew. Chem. 106 (1994) 1960; Angew. Chem., Int. Ed. Engl. 33 (1994) 1875.
[44] P. Miele, J.D. Foulen, N. Hovnanian, J. Durand, L. Cot, J. Solid State Inorg. Chem. 29 (1992) 573.
[45] F.A. Cotton, G. Wilkinson, Advanced Inorganic Chemistry, 5th ed., Wiley, New York, 1988.
[46] J.E. Huheey, Inorganic Chemistry, 3rd ed., Harper and Row, New York, 1983.
[47] G. van Koten, J.G. Noltes, in: G. Wilkinson, F.G.A. Stone, E.W. Abel (Eds.), Comprehensive Organometallic Chemistry, Pergamon, London, 1982, p. 709.
[48] S.C. James, N.C. Norman, A.G. Orpen, M.J. Quayle, J. Chem. Soc., Dalton Trans. (1997) 1455.
[49] M.A. Beswick, N. Choi, A.D. Hopkins, M. McPartlin, M.A. Paver, D.S. Wright, J. Chem. Soc., Chem. Commun., in press.
[50] W. Neubert, H. Pritzkow, H.P. Latscha, Angew. Chem. 100 (1988) 298; Angew. Chem., Int. Ed. Engl. 27 (1988) 287.
[51] R.N. Grimes, Compre. Organomet. Chem.; Transition Metallacarboranes, in: C.E. Housecroft (Ed.), Pergamon. 1995, vol. 1, Ch. 9, p. 373.
[52] A.R. Oki, H. Zhang, N.S. Hosmane, Angew. Chem. 104 (1992) 441; Angew. Chem., Int. Ed. Engl. 31 (1992) 432.
[53] A.R. Oki, H. Zhang, N.S. Hosmane, H. Ro, W.E. Hatfield, J. Am. Chem. Soc. 113 (1991) 8531.
[54] R.E. Allan, M.A. Beswick, A.J. Edwards, et al., J. Chem. Soc., Dalton Trans. (1995) 1991.
[55] R.E. Allan, PhD Thesis, Cambridge University, 1997.
[56] M. Veith, O. Recktenwald, Z. Naturforsch. B38 (1983) 1054.
[57] M. Veith, G. Schlemmer, Chem. Ber. 115 (1982) 2141.
[58] M. Veith, M. Grosser, Z. Naturforsch. B37 (1982) 1375.
[59] H. Chen, R.A. Bartlett, H.V.R. Dias, M.M. Olmstead, P.P. Power, Inorg. Chem. 30 (1991) 3390.
[60] R.E. Allan, M.A. Beswick, G.R. Coggen, P.R. Raithby, A.E.H. Wheatley, D.S. Wright, Inorg. Chem. 35 (1997) 2502.
[61] M. Veith, Angew. Chem. 99 (1987) 1; Angew. Chem., Int. Ed. Engl. 26 (1987) 1.
[62] M. Veith, M.-L. Sommer, D. Jäger, Chem. Ber. 112 (1979) 2581.
[63] R.A. Bartlett, P.P. Power, J. Am. Chem. Soc. 112 (1990) 3660.
[64] M. Veith, W. Frank, Angew. Chem. 23 (1984) 158; Angew. Chem., Int. Ed. Engl. 96 (1984) 163.
[65] R.E. Allan, M.A. Beswick, N. Feeder et al., Inorg. Chem., in press.
[66] R.E. Allan, M.A. Beswick, N.L. Cromhout, et al., J. Chem. Soc., Chem. Commun. (1996) 1501.
[67] K.M. Waggoner, P.P. Power, J. Am. Chem. Soc. 113 (1991) 3385.
[68] R.E. Allan, M.A. Beswick, P.R. Raithby, A. Steiner, D.S. Wright, J. Chem. Soc., Dalton Trans. (1996) 4153.
[69] M. Westhausen, W. Schwarz, Z. Anorg. Allg. Chem. 622 (1996) 903.
[70] R.L. Wells, A.P. Purdy, A.T. McPhail, C.G. Pitt, J. Chem. Soc., Chem. Comm. (1986) 487.
[71] A.H. Cowley, R.A. Jones, M.A. Mardones, J.L. Atwood, S.G. Bott, Angew. Chem. 103 (1991) 1163; Angew. Chem., Int. Ed. Engl. 30 (1991) 1141.
[72] K.M. Waggoner, S. Parkin, D.C. Pestana, H. Hope, P.P. Power, J. Am. Chem. Soc. 113 (1991) 3597.
[73] A.R. Barron, P.P. Power, Angew. Chem. 103 (1991) 1403; Angew. Chem., Int. Ed. Engl. 30 (1991) 1353.
[74] D.A. Atwood, A.H. Cowley, R.A. Jones, M.A. Mardones, J. Organomet. Chem. 449 (1993) C1.
[75] A.H. Cowley, R.A. Jones, M.A. Mardones, J.L. Atwood, S.G. Bott, Angew. Chem. 102 (1990) 1504; Angew. Chem., Int. Ed. Engl. 29 (1990) 1409.

[76] M.P. Petrie, P.P. Power, Organometallics 12 (1993) 1592.
[77] R.E. Allan, M.A. Beswick, M.K. Davies, P.R. Raithby, A. Steiner, D.S. Wright, J. Organomet. Chem., in press.
[78] M.A. Beswick, M.K. Davies, M.A. Paver, P.R. Raithby, A. Steiner, D.S. Wright, Angew. Chem. 108 (1996) 1660; Angew. Chem., Int. Ed. Engl. 35 (1996) 1508.
[79] R. Fleischer, S. Freitag, F. Pauer, D. Stalke, Angew. Chem. 108 (1996) 208; Angew. Chem., Int. Ed. Engl. 35 (1996) 204.
[80] A. Gieren, P. Narayanan, Acta. Crystallogr. A31 (1975) 120.
[81] H.W. Roesky, W. Schneider, W.S. Sheldrick, J. Chem. Soc., Chem. Commun. (1981) 1013.
[82] M. Björgvinsson, H.W. Roesky, F. Pauer, G.M. Sheldrick, Chem. Ber. 125 (1992) 767.
[83] T. Chivers, M. Parvez, G. Schatte, Inorg. Chem. 35 (1996) 4094.
[84] N.J. Bremer, A.B. Cutliffe, M.F. Farona, W.G. Kofron, J. Chem. Soc. (1971) 3264.
[85] T. Chivers, X. Gai, M. Parvez, Angew. Chem. 107 (1995) 2756; Angew. Chem., Int. Ed. Engl. 34 (1995) 2549.
[86] R.E. Allan, H. Gornitzka, J. Karcher, et al., J. Chem. Soc., Dalton Trans. (1996) 1727.
[87] M. Bjorgvinsson, H.W. Roesky, F. Pauer, D. Stalke, G.M. Sheldrick, Angew. Chem. 103 (1991) 1671; Angew. Chem., Int. Ed. Engl. 30 (1991) 1677.
[88] M. Bjorgvinson, H.W. Roesky, F. Pauer, D. Stalke, G.M. Sheldrick, Inorg. Chem. 29 (1990) 5140.
[89] M. Bjorgvinson, H.W. Roesky, F. Pauer, D. Stalke, G.M. Sheldrick, Eur. J. Solid State Chem. 29 (1992) 759.
[90] M.A. Beswick, C.N. Harmer, A.D. Hopkins, M. McPartlin, D. S. Wright, unpublished results (patent pending), Science, in press.